

Norwegian University  
of Life Sciences

**Master Thesis 2018 60 ECTS**

Faculty of Environmental Science and Natural Resources Management

# **Speciation and mobility of particle-associated radiocesium in soils and pond sediments from Fukushima, Japan**

**Abednego Tetteh**

MSc. Radioecology  
Department of Environmental Science



## Abstract

The Fukushima Daiichi Nuclear Power Plant (FDNPP) accident that occurred in March 2011 at the nuclear facilities of units 1, 2 and 3 in Japan resulted in the release of radioactive cesium ( $^{137}\text{Cs}$ ) containing particles. In this work, the speciation and mobility of particle associated radiocesium was investigated by sequential extraction, digital autoradiography and leaching experiment (with 0.16 M HCl) on contaminated soil and pond sediment samples collected from areas close (approximately 11 km) to the damaged reactors. Upon screening samples with digital autoradiography, very heterogeneous distributions of hotspots were encountered in all investigated samples, indicating the presence of radioactive particles. The number of particles reflects the direction of the plume from the reactors. In addition, the radioactive particles were found to exert certain influence on  $^{137}\text{Cs}$  mobility and bioavailability. The results from sequential extractions showed that  $^{137}\text{Cs}$  in soils and pond sediments remain largely irreversibly bound and is associated to inert fractions. Moreover, upon subjecting a small soil and sediment samples to simulated gastrointestinal fluid (0.16 M HCl) extractions for 65 hours,  $< 3\%$  of  $^{137}\text{Cs}$  was leached indicating a low degree of potential mobility and bioavailability. From the study it was concluded that  $^{137}\text{Cs}$  in soils and pond sediments in the Fukushima area is of relatively low mobility and potential bioavailability.

## Acknowledgment

I wish to express my greatest appreciation to the Almighty God for seeing me through another level of my education. It was really a challenging moment for me at a point in time, but the grace and mercy of God saw me through. To Him be all the glory and honour.

My sincere thanks also goes to Associate Professor Ole Christian Lind (my main supervisor), for his immense contribution and technical guidance. I am grateful for your patience and for giving generously of your time at a critical moment such that you allowed me to make 11th-hour updates to the text.

Special thanks go to Dr. Estela Reinoso-Maset (my co-supervisor) for her intellectual stimulation and constructive criticisms that has been very helpful for my progress. Her numerous corrections to the text helped to improve this thesis. Any remaining errors and omissions are to be laid squarely at my door.

I received a great deal of support and assistance from several members of staff at CERAD in carrying out this thesis. I am greatly indebted to Senior Engineer Marit Nandrup Pettersen for her invaluable assistance and guidance at the Isotope Laboratory, especially with the soil analysis and grain size determination.

A special note of thanks is due to Dr. Ing. Frits Steenhuisen (University of Groningen) for providing the location maps and accompanying data. Moreover, I want to thank all the people who participated in the fieldwork at Fukushima in 2016, from which I obtained my samples. Thanks also go to the director and staff at the Centre for Environmental Radioactivity (CERAD) of the University of Life Sciences (NMBU), for giving me the opportunity to work on this project.

I would not have been able to complete this thesis without the enthusiastic support of my family. My wife, Dr. Mercy Afadzi, provided emotional ballast with her love and constant encouragement. Danita, my adorable daughter, gave me a reason to get up in the morning.

## Contents

Abstract.....	1
Acknowledgment.....	2
List of Figures.....	5
List of Tables .....	6
<b>1. INTRODUCTION .....</b>	<b>7</b>
1.2. Hypothesis.....	8
1.3. Objectives .....	8
<b>2. LITERATURE REVIEW .....</b>	<b>10</b>
2.1. The Fukushima Daiichi Nuclear Power Plant (FDNPP) accident .....	10
2.2. Formation of radiocesium particles in FDNPP .....	12
2.3. Particles of Fukushima origin.....	13
2.4. Radiological situation in the Fukushima Exclusion Zone (FEZ).....	14
2.5. Speciation.....	15
2.5.1. Speciation techniques.....	18
2.5.2. Radioactive particles.....	19
2.5.3. Importance of considering radioactive particles .....	20
2.6. Chemical, Physical and Environmental Properties of Cesium .....	21
2.6.1. Cesium.....	21
2.6.2. Physical and chemical properties .....	23
2.6.3. Factors influencing cesium species in terrestrial and aquatic systems .....	24
<b>3. MATERIALS AND METHODS.....</b>	<b>30</b>
3.1. Site and Sample Description .....	30
3.2. Soil and Sediment Characterization.....	33
3.2.1. Sample preparation.....	33
3.2.2. pH measurement .....	33
3.2.3. Grain size distribution .....	34
3.2.4. Determination of organic matter content.....	34
3.3. Sequential extraction .....	34
3.4. Leaching with 0.16 M HCl .....	38
3.5. Gamma measurements .....	40
3.5.1. Interaction of gamma rays with matter.....	42
3.6. Intercomparison of methods .....	43

<b>3.7. Digital autoradiography .....</b>	<b>44</b>
3.7.1. <i>Image acquisition, processing and analysis.....</i>	<i>44</i>
<b>3.8. Statistical analysis .....</b>	<b>46</b>
<b>4. RESULTS AND DISCUSSION.....</b>	<b>47</b>
4.1. Soil and sediment characteristics.....	47
4.2. Distribution of $^{137}\text{Cs}$ in different grain sizes .....	48
4.3. Distribution of $^{137}\text{Cs}$ in different layers of soils and sediments .....	50
4.4. Leaching behaviour of 0.16 M HCl .....	53
4.5. Sequential extraction of $^{137}\text{Cs}$ from soils and sediments .....	55
4.7. Assessing the influence of soil/sediment characteristics on binding mechanism of $^{137}\text{Cs}$ ...	62
4.8. Influence of radioactive particle on $^{137}\text{Cs}$ speciation.....	63
<b>5. CONCLUSION .....</b>	<b>65</b>
<b>References .....</b>	<b>66</b>
<b>Appendix 1A Results obtained for the sequential extraction.....</b>	<b>73</b>

## List of Figures

Figure 1. Layout of the Fukushima Daiichi Nuclear Power Station (FDNPS) and its fixed automatic monitoring posts (MP). Adapted from UNSCEAR (2014).....	11
Figure 2: The deposition density of $^{137}\text{Cs}$ based on data from the MEXT ground survey adjusted to 14 June 2011. Adapted from UNSCEAR (2014) .....	12
Figure 3: Categorisation of radionuclides according to its speciation. Adapted from Salbu (2007).....	17
Figure 4: Simplified decay diagram of $^{137}\text{Cs}$ . About 94% of Cs nuclei decay to an excited state of ( $^{137}\text{Ba}$ )* which subsequently decays by emitting $\gamma$ –radiation. Adapted from Atwood (2013) .....	23
Figure 5: Pathways of exposure following the release of $^{137}\text{Cs}$ to the environment. Adapted from UNSCEAR (2014) .....	29
Figure 6: Map showing the sampling locations with station numbers and deposition isolines of the 11 km FEZ from the reactors. The colour isolines represent the $^{137}\text{Cs}$ deposition in $\text{kBq}/\text{m}^2$ .....	31
Figure 7: Experimental setup for the sequential extraction; plastic pipette beside funnels with inserted filters, placed in a funnel holder over sample vials, and centrifuge tubes in a rack. ....	37
Figure 8: Gamma measurements on NaI detector (PerkinElmer Wizard2® 2480 Automatic Gamma Counter).....	41
Figure 9: Effect of counting time on counting uncertainty: (a) activities $<500\text{DPM}$ (b) $>1000\text{DPM}$ .....	42
Figure 10: Comparison of $^{137}\text{Cs}$ measurements between NaI and Ge detectors .....	43
Figure 11: Overview of processes involved in acquiring image of particles using digital autoradiography. From top (left - prepared sample, right - imaging plate) and bottom (left – exposure cassette, right – digital phosphor plate scanner).....	45
Figure 12: The content of $^{137}\text{Cs}$ in different grain sizes in the selected sites. Site 6, 7, 10, 16A and 17 are soils while 16B and 18 are sediment .....	48
Figure 13. Proportion of $^{137}\text{Cs}$ contained in the different grain sizes at different levels of soils (A) and sediments (Band C) .....	52
Figure 14: Proportion of $^{137}\text{Cs}$ leached in (A) total samples before size-segregation, (B) sand fraction, (C) silt fraction, and (D) clay fraction. Site 6, 7, 10, 16A and 17 are soils while 16B and 18 are sediments .....	54
Figure 15: : Percentage distribution of $^{137}\text{Cs}$ in the fractions from sequential extraction of five soils and two fresh sediments from the 11 km zone in FDNPP area. ....	55
Figure 16: Fractionation of $^{137}\text{Cs}$ in soils and sediments as a fraction of the total activity following sequential extraction. Site 7, 8, 10,13 and 16A are soils while 16B and 18 are sediments .....	57
Figure 17: Representative autoradiogram showing hotspots, along with its surface plots.....	58
Figure 18: Number of particles per gram of dry mass as a function of distance and direction to the reactor in (a) total and (b) residue form sequential extraction. The numbers are for the various sites, while the colour represent direction.....	61
Figure 19: Correlation between Activity concentration in residuals and number of particles from residuals after sequential extraction.....	64

## List of Tables

<i>Table 1: Common cesium radioisotopes produced by nuclear fission and activation (Adapted from Atwood (2013)</i>	22
<i>Table 2: Factors influencing aquatic transport (Kathren (1984) .....</i>	25
<i>Table 3: Retention time-scale indicating the biological and environmental half-lives of <sup>137</sup>Cs in organisms and environmental objects. Adapted from Dubchak (2017) .....</i>	28
<i>Table 4: Information regarding samples and sampling location.....</i>	32
<i>Table 5: Summary of sequential extraction procedure carried out in the laboratory .....</i>	38
<i>Table 6: Details of soil and sediment samples subjected to sequential extraction procedure.....</i>	49
<i>Table 7: The number of radioactive particles per gram of dry mass of sample before (total) and after (residue) sequention extraction (S.E).....</i>	60

## 1. INTRODUCTION

The massive earthquake that triggered tsunami, struck northeast Japan on March 11, 2011, causing extensive damage to the Fukushima Daiichi Nuclear Power Plant (FDNPP) and resulted in the release of high levels of radiocesium ( $^{134}\text{Cs}$ ,  $^{135}\text{Cs}$ ,  $^{137}\text{Cs}$ ,) among other radionuclides in the vicinity of the damaged nuclear reactor and beyond (Chino et al., 2011; Kinoshita et al., 2011; Yasunari et al., 2011). Radiocesium deposited in the Fukushima Prefecture occurred via wet and dry deposition, significantly contaminating large areas of the northwestern region of the Fukushima Daiichi Nuclear Power Plant (FDNPP) with contamination reaching 50-70 km long and 20 km wide (Hirose, 2012; Saito et al., 2015). As is expected following a severe nuclear event such as FDNPP accident, a significant portion of radionuclides released were in the form of radioactive particles (Salbu et al., 2015). These radioactive particles were deposited at various distances from the accident site contaminating forests, ponds, rivers, fields and residences, and these particles could persist in the environment for a long time, with the potential for adverse health effects. The presence of radioactive particles can give rise to inhomogeneous distribution of radionuclides in the environment (IAEA, 2011a) as well as carry substantial amount of radioactivity, which can be subjected to re-suspension, atmospheric transport and water transport (Salbu et al., 2001b).

The nature of the FDNPP accident has resulted in creating a complex radioactive contaminated system. Furthermore, speciation of radiocesium in Fukushima has not been clearly defined. Despite several research conducted, many knowledge gaps hinder our understanding of the behaviour of particles, posing a challenge to predict how changes in the environment can affect particle weathering. Few studies have focused on the behaviour of radioactive particles in the Fukushima Exclusion Zone (FEZ). To predict the future dynamics of particle bearing radiocesium, continuous research would be deemed beneficial. Research is clearly needed to address the challenges related to knowledge on particle characteristics, weathering and leaching, since they are essential for ecosystem transfer, as well as biological significance of particles. Although sensitivity analysis of assessment models usually consider dissolution rates, distribution coefficients ( $K_d$ ) and biological concentration factors as the most sensitive parameters that contribute to large uncertainties in impact assessments (Oughton & Kashparov, 2009; Skipperud et al., 2000a), there is a need to assess the impact of radioactive particles on the

mobility and bioavailability of radiocesium. Moreover, the particle source characteristics and environmental conditions could also provide a useful link to weathering and dissolution rates.

In this work, an investigation has been undertaken to study how radioactive particles can influence mobility and bioavailability of radiocesium (specifically,  $^{137}\text{Cs}$ ). This is based on the fact that  $^{137}\text{Cs}$  is present in different physico-chemical forms, thereby influencing the environmental behaviour. Different techniques and measurements were used in this work. A sequential extraction procedure was applied on 5 soil and 2 sediment samples from 11 km within the Fukushima Exclusion Zone (FEZ) contaminated by radioactive particles to study the speciation of  $^{137}\text{Cs}$  in order to determine concentrations of biologically important trace  $^{137}\text{Cs}$  and to provide relevant information on the mobility and bioavailability of  $^{137}\text{Cs}$ . Besides, the sequential extraction procedure revealed information regarding the association of  $^{137}\text{Cs}$  with soil components. Leaching of particle contaminated soil and sediments with 0.16 M HCl mimicking simulated stomach juice also provided a valuable insight on solubility and bioavailability of  $^{137}\text{Cs}$ . By screening samples for heterogeneities using digital phosphor imaging, the presence and distribution of potential radioactive particles were detected and quantified for all investigated samples. The distribution of  $^{137}\text{Cs}$  in different grain-size fractions was also determined.

## **1.2. Hypothesis**

This work is based on the following hypothesis:

1. The speciation of  $^{137}\text{Cs}$  in the 11 km FEZ is different due to the presence of radioactive particles.
2. The non-binding of  $^{137}\text{Cs}$  to clay minerals suggest that inert radioactive particles are controlling the mobility and bioavailability of radiocesium in the 11 km FEZ
3. Identification of heterogeneous distribution of hotspots suggests possible release of radioactive particles, since severe nuclear events does not result in homogenous distribution of particles.

## **1.3. Objectives**

The objectives of this research are as follows:

- To investigate the binding of Cs in soil and pond sediments in the FEZ.

- To investigate the potential mobility and bioavailability of Cs in soil and pond sediments in FEZ.
- To evaluate effect of soil and sediment characteristics on the behaviour of  $^{137}\text{Cs}$ .
- To quantify heterogeneity in the radioactive particles

## 2. LITERATURE REVIEW

### 2.1. The Fukushima Daiichi Nuclear Power Plant (FDNPP) accident

The Fukushima Daiichi Nuclear Power Plant (FDNPP) accident is a triple disaster that occurred on March 11, 2011 in Fukushima Prefecture of the Tōhoku region in Japan, when an offshore earthquake of magnitude 9.0 triggered a devastating tsunami, leading to power losses, overheating, and subsequent release of large amounts of radioactive materials to the environment. The sequence of events is described in a report prepared by the United Nations Scientific Committee on the Effects of Atomic Radiation (UNSCEAR, 2014). It was reported that Units 1–3 of Fukushima Daiichi Nuclear Power Station (FDNPS) were in normal operation when the earthquake occurred off the eastern coast of Japan at 14:46 Japan Standard Time (JST) on 11 March 2011. The three other reactors (Units 4–6) had already been shut down due to periodic maintenance and refuelling operations, for which Unit 4 had been completely defuelled. A layout of the FDNPS, along with its fixed automatic monitoring posts (MP) is shown in Figure 1. As soon as the seismic activity hit the area, Units 1–3 immediately underwent emergency shutdown. Then, the FDNPS lost all connection with its off-site electricity supply due to seismic tremors damaging the power transmission grids. Although emergency diesel generators were automatically activated to provide backup power for cooling the reactors, a tsunami wave with an estimated maximum height of about 15 m over the 6 m seawall inundated the FDNPS site in less than one hour, and flooded a number of emergency safety systems. This situation caused Units 1, 2 and 4 to lose all power while Unit 3 initially lost its AC power followed by the loss of DC power before dawn of 13 March 2011. Unit 5 also lost all AC power, however, Unit 6 had electricity supplied from an air-cooled emergency diesel generator. The ultimate result was the melting of the reactor cores of Units 1, 2 and 3, which was accompanied by the substantial release of radioactive material into the atmosphere and the ocean.

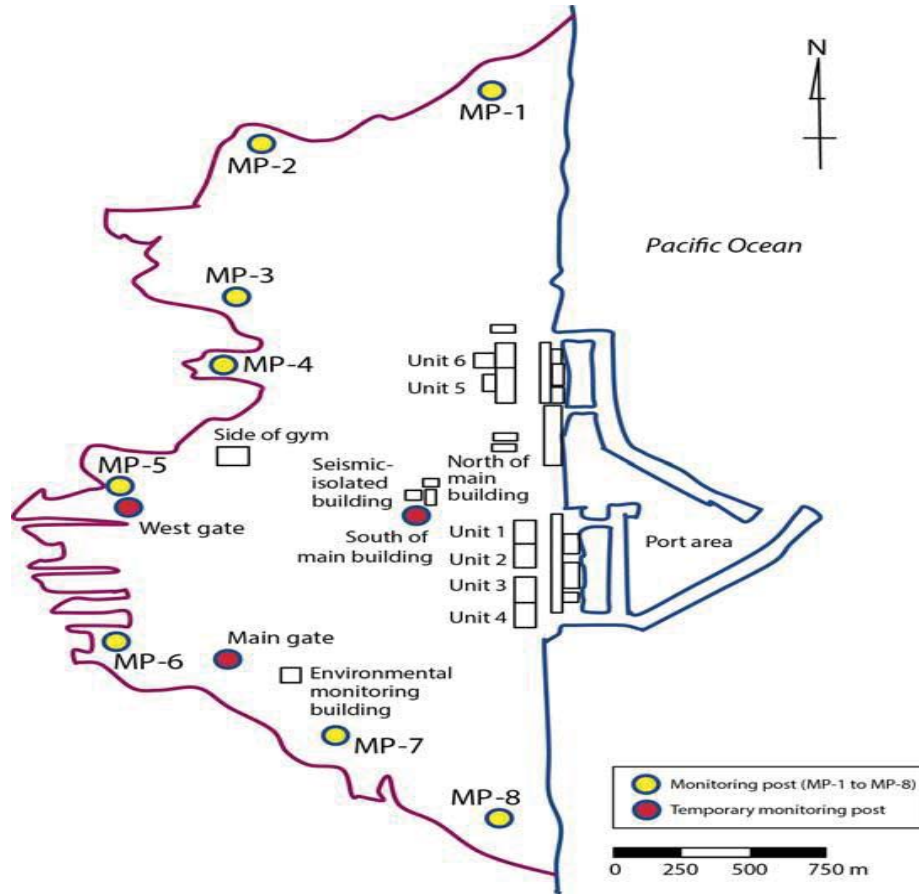


Figure 1. Layout of the Fukushima Daiichi Nuclear Power Station (FDNPS) and its fixed automatic monitoring posts (MP). Adapted from UNSCEAR (2014)

Following the accident, about  $9 \times 10^{17}$  Bq of radioactive substances mainly fission and activation products were released from the molten fuel in the reactors (generally as aerosols or in a gaseous form) into the environment. This resulted in the significant contamination of an area of about 30 km around the damaged FDNPP referred to as the Fukushima Exclusion Zone (FEZ) (Gupta & Walther, 2017). Due to the nature of the accident, the most significant contribution to radioactive contamination were made by radiocesium with about  $1 \times 10^{16}$  Bq of  $^{137}\text{Cs}$ . The deposition density of  $^{137}\text{Cs}$  averaged by district within Fukushima Prefecture and some districts in neighbouring prefectures is presented in Figure 2

Since the FDNPP accident in 2011, the radioecological situation in the FEZ and neighbouring areas are expected to have undergone some changes. It is possible the FEZ might have been subjected to secondary contamination resulting from radioactive soils and sediments transported

by surface run off and wind from steep slopes to the ponds and other areas. As a result of these processes in addition to different accident scenarios likely to have occurred in the three damaged reactors, a complicated radioecological situation is assumed to have developed in the FEZ.

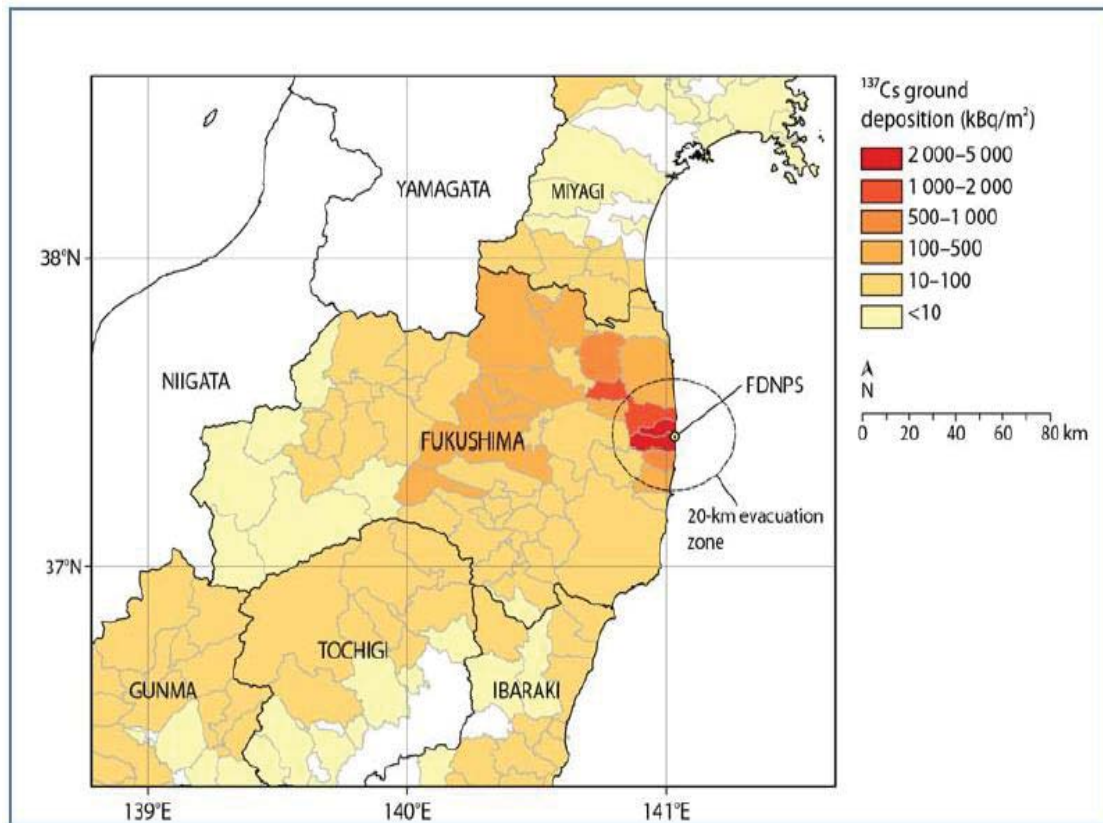


Figure 2: The deposition density of  $^{137}\text{Cs}$  based on data from the MEXT ground survey adjusted to 14 June 2011. Adapted from UNSCEAR (2014)

## 2.2. Formation of radiocesium particles in FDNPP

Formation of cesium containing radioactive particles is as a result of critical (e.g. explosions, fires) or subcritical (e.g. corrosion processes) destruction of fuel matrices, and by clustering, condensation or interactions of radionuclides with available particle surfaces during release and dispersion (Salbu et al., 2015). It is believed that at high temperature and pressure conditions such as a nuclear explosion, there will be liquefaction of materials, enabling volatile radionuclides like cesium to preferentially be released as gases. These volatile radionuclides can settle on available surfaces such as soot, fly ash, and airborne dust forming condensation

particles upon cooling, as observed following the Chernobyl accident (IAEA, 2011b). It must be emphasized that under low temperature and pressure conditions such as fire, the characteristics of particles released will be different from those released at high temperature and pressure conditions during reactor explosion (Salbu, 2011).

In the case of the FDNPP accident, the loss of electrical power resulted in the loss of cooling to the reactors. Heat generated by the radioactive materials in the reactor core without any source of cooling, couple with mounting pressure inside the reactor vessels led to the core damage. Water or steam generated by injection pumps in direct contact with the over-heated fuel assemblies might have reacted with zirconium of the fuel cladding to produce hydrogen gas. Accumulation of this hydrogen gas in the upper part of the reactor buildings or secondary containment ignited, producing explosions in the Unit 1 and Unit 3 reactor buildings on 12 and 14 March, respectively. It is assumed that hydrogen gas generated in Unit 3 migrated into the Unit 4 reactor building, causing explosion and damage there on 15 March 2011 (UNSCEAR, 2014). The chemical composition of aerosols formed by revaporisation and subsequent condensation of fission products is still a subject of further enquiry. A range of  $^{137}\text{Cs}$  species could be encountered at FEZ given the complex nature of the accident.

### **2.3. Particles of Fukushima origin**

As a consequence of the FDNPP accident, it is reported that cesium containing particles were released to the environment (Gupta & Walther, 2017). A growing amount of data on cesium and other radionuclides in soils and sediments from FDNPP area has been generated following the accident. Since the system is complex, knowledge about speciation is still limited and further work is needed to arrive at a better understanding. Radiocesium in soil and sediment from FDNPP area may be present due to dry and wet deposition, weathering and leaching of fuel particles, or the migration of run-off water with enhanced concentrations of radiocesium. To date, there is still debate about the source of Fukushima particles. After the FDNPP accident, some researchers (Abe et al., 2014; Adachi et al., 2013; Miyamoto et al., 2014; Satou et al., 2016) have claimed finding radioactive particles containing radiocesium, uranium and other stable elements representative of fuel and reactor materials from the damaged Fukushima reactors. Meanwhile, particles of similar properties have also been identified in those originating

from coal combustion (Ault et al., 2012). Other authors also suggest that radiocesium containing particles might have originated from condensation processes, assuming that the particles are water-soluble and washable by precipitation.

#### **2.4. Radiological situation in the Fukushima Exclusion Zone (FEZ)**

Several authors have reported on radiocesium to be a major source of radiation in the Fukushima Exclusion Zone (FEZ), such that estimation of its resuspension and future predictions in the terrestrial and aquatic environment should be prioritized (Konoplev et al., 2016; Wakiyama et al., 2017). Exposure to particles bearing radiocesium poses potential risk to organisms due to its radiological and chemical toxicity. Research (Beresford et al., 1989; Beresford & Howard, 1991; Beresford et al., 1992; Beresford et al., 2000; Howard et al., 1991; Itoh et al., 2014; Jaeschke et al., 2015) have shown that radioactive contaminated soils and particles can be ingested by organisms, posing a potential risk to humans who are at the apex of the food chain.

Fukushima Prefecture is known for having over 3700 individual ponds of varying sizes, which are predominantly used for irrigation purposes (Wakiyama et al., 2017). Likewise, Fukushima watersheds are characterized by hills with steep slopes, and secondary contamination may occur due to radioactive contamination being carried in surface run off to cleaner areas. Although some studies have been conducted by the Japanese authorities on  $^{137}\text{Cs}$  activity concentrations in water and bottom sediments of 2679 ponds, these were mainly related to temporal trends and fluctuations (Kubota et al., 2015). However, only limited studies on the behavior of radiocesium in the ponds bordering the near zone of the reactor, where fallout was greatest has been studied.

Pioneering studies conducted after the Chernobyl nuclear power plant (ChNPP) accident has shown that closed and semi closed water bodies (such as lakes, reservoirs and ponds) characterized by high organic matter content and increased ammonium concentrations in water, were the most sensitive environments to radiocesium contamination (Comans et al., 1989; Konoplev et al., 1998; Smith et al., 2005). It was also suggested by Comans et al. (1989) that radiocesium can be mobilized from lacustrine anoxic sediments leading to seasonal cycling of  $^{137}\text{Cs}$ , with the possibility to influence the distribution coefficient ( $K_d$ ). While particle growth processes are expected to increase the  $K_d$  with time, remobilization will decrease the  $K_d$  with

time. The above processes could result in a complicated behaviour of radiocesium in Fukushima. Therefore the mechanism of radiocesium behaviour in Fukushima ponds and soils need to be understood for the sake of restoring the region, as well as for emergency preparedness of future nuclear accidents.

Radiocesium associated with colloids (1-10 nm) may be formed in these aquatic systems due to low temperature conditions favouring the presence of colloidal material, and the surfaces of colloids in natural waters (usually negatively charged, partly due to organic coatings), act as carriers for cationic species (Guillén et al., 2012; Kathren, 1984). A change in chemical conditions in these aquatic systems may influence the stability of colloids. Interaction of radiocesium with different chemicals and particulates present in the water or attachment to different fractions of size and charge can lead to precipitation and subsequent sedimentation. Moreover, aggregation of colloids can result in sedimentation, subsequently, radiocesium species can later be mobilized from solid surfaces due to increased ionic strength.

Soil and sediments can act as sinks for deposited radioactive particles. Conversely, particle contaminated soil and sediments can act as potential diffuse sources in the future. Thus, knowledge with respect to particle characteristics and processes influencing particle weathering and remobilization of associated radionuclides is needed to assess long-term impact from radioactive particle contamination. Research indicates that after deposition, there will be delay in the ecosystem transfer of particle associated radionuclides in comparison with the mobile radionuclide species until particle weathering and remobilization of associated radionuclides occur. Meanwhile, by conducting analysis using  $^{90}\text{Sr}$ , Salbu et al. (2017) demonstrated that particle weathering do occur, and that particle associated radionuclides can be remobilized, emphasizing the biological importance of radioactive particles .

## **2.5. Speciation**

Assessing the long term environmental impact of radioactive contamination of ecosystems require information on source terms including radionuclide speciation, mobility and biological uptake (Skipperud et al., 2000a). Besides, speciation has shown itself remarkably vital in assessing risk, because speciation dictates the weathering, mobilization, transfer and long term

behaviour in the ecosystem (Admon, 2009; Salbu et al., 2004). In order to understand speciation, it is important to have a definition of what constitutes radionuclide species. Radionuclide species are defined according to their physico-chemical properties such as molecular mass, charge properties, oxidation state, valence, structure, complexing ability among others.

Usually, radionuclides released from a source to the environment can be present in different physico-chemical forms, ranging from low molecular mass (LMM) ions, molecules and complexes to polymers, nanoparticles, colloids, particles and fragments (Salbu, 2007) (Figure 3). That is why it is important to identify all these forms to make a meaningful impact assessment, as total concentrations do not provide such needed information. Speciation therefore is the distribution of a radionuclide among these different physico-chemical forms (Salbu, 2009b). It is believed that LMM species like ions, molecules and complexes (e.g. cations, anions and neutrals) are mobile and bioavailable, and can be transported across cell membranes by active uptake. These are entities less than about 1 nm (1-10 kDa). Nanoparticles, colloids, polymers and pseudocolloids known as high molecular mass (HMM) species are considered as localized aggregates in the size range of 1 nm–0.45µm. They are believed to be mobile, and poses specific properties that may enable them to pass biological membranes by passive uptake, and can be retained in filtering organisms or be ingested by aquatic organisms. Particles (i.e. entities in the size range 0.45µm–2mm) are usually considered inert can be retained in soils and sediments and grazing mammals. Larger radioactive entities about 2 mm are called fragments. From the foregoing, if mobile species are present as the dominant species, the ecosystem transfer is relatively fast, however, if particles are the dominant part of the release, the ecosystem transfer will be delayed.

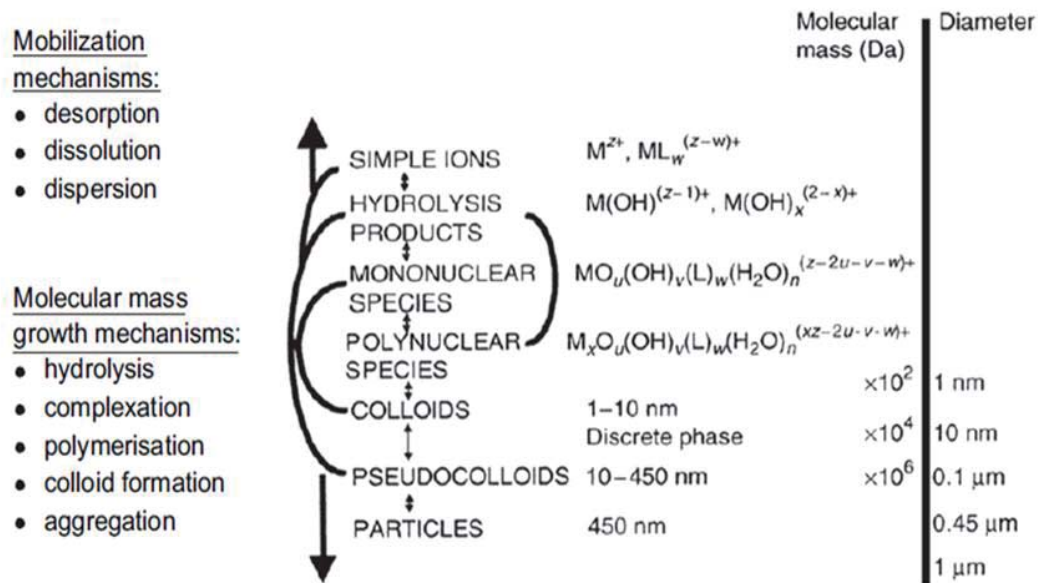


Figure 3: Categorisation of radionuclides according to its speciation. Adapted from Salbu (2007)

Since environmental systems are dynamic, molecular mass growth mechanisms such as hydrolysis, polymerization, and colloid aggregation reduce the mobility and bioavailability over time (Salbu, 2007). On the contrary, radionuclides can be mobilized and transformed to a more bioavailable form due to mobilization processes such as desorption, dispersion, dissolution or particle weathering (Salbu, 2009a). With time, the speciation of radionuclides originally deposited are liable to change due to interactions with constituents in soils and sediments. It follows that the mobility of LMM species can be reduced due to interactions with humic substances or clays, while the presence of LMM organic acids may mobilize radionuclides leading to the formation of LMM complexes. In addition, weathering of particles will lead to remobilization of associated particles, resulting in the increase of ecosystem transfer with time (Kashparov et al., 1999).

As indicated earlier, the speciation of radionuclides deposited after a nuclear event depends on source term and release scenario characteristics, transport and dispersion mechanisms and ecosystem properties (Salbu & Skipperud, 2009). It follows that particle characteristics such as elemental composition depend on the source, while characteristics such as particle size distribution, structure, and oxidation state that influence ecosystem transfer depend on the release

scenarios. Thus source and release term is an essential input data to dispersion and transport models. Traditionally, the moderator material, the fraction of radionuclides released, the activity concentration of radionuclides deposited in the environment, or the inventory activity concentrations of radionuclides are included in the source term (Whicker et al., 1999). The release scenario include among others, temperature, pressure, redox conditions that influence particle characteristics of biological significance (Salbu et al., 2001a).

The release of radiocesium from Fukushima soils and sediments is of environmental concern given the enormous benefits of the aquatic systems and land use in the area. Also, the speciation can substantially affect the bioavailability of radiocesium for bottom feeding organisms. Research showed that radiocesium speciation in Chernobyl fallout following the accident was dependent on the distance from the damaged ChNPP, as fuel particles formed the main deposition close to the reactor, with fine condensation particles carried in a long distance transport (Konoplev, 1998; Wakiyama et al., 2017). Likewise, the knowledge obtained from speciation may contribute to the characterization of sources of radioactive pollution for the receiving water body.

#### *2.5.1. Speciation techniques*

Salbu et al. (2017) has suggested that for areas affected by particle contamination, the consideration of radionuclide species including particles and description of their interactions and transfer will significantly reduce the overall uncertainties in impact and risk assessments. The application of analytical techniques to identify and quantify one or more individual radionuclide species in a sample is known as speciation analysis. Speciation analysis can be done in situ, at site, on line, or at laboratory by applying fractionation techniques prior to measurements. For radionuclide species in soils and sediments, isolation of particle fractions can be done by wet or dry sieving prior to analyses, while sequential extraction techniques can be used to distinguish between reversibly and irreversibly bound fractions (Salbu & Krekling, 1998). Furthermore, characterization of particles isolated from soils and sediments can be achieved by using non-destructive solid state speciation techniques such as electron microscopy techniques, synchrotron based micro X-ray techniques and laser techniques (Salbu, Brit, 2000; Salbu et al., 2001a). Other potential solid-state speciation techniques that can be used include  $\mu$ -PIXE and SIMS, providing

information on distribution of elements within particles,  $\mu$ -RAMAN and electron diffraction, which provide structural information, and electron energy loss spectroscopy (EELS) providing information on oxidation states, and nuclear magnetic resonance spectroscopy.

#### *2.5.2. Radioactive particles*

According to IAEA (2011a), radioactive particles are localized aggregates of radioactive atoms that may contain significant activity concentrations, and give rise to inhomogeneous distribution of radionuclides significantly different from that of the matrix background. These are radioactive entities typically in the size range of 0.45 $\mu$ m–2mm (Salbu, 2013). Since severe nuclear events does not result in uniform distribution of radionuclides, observation of inhomogeneous distribution of radionuclides (i.e. localized heterogeneities) in soil and sediment samples can be a good indication of the presence of radioactive particles.

Single radioactive particles are known to carry a great deal of information regarding radiological, chemical and metallurgical history, and clues pertaining to release-scenario (Admon, 2009). Besides, the physico-chemical characteristics of every individual particle can reveal its mobilization and long-term behavior in the ecosystem. It must be emphasized that for acute respiration and skin doses, information such as particle size distribution, composition and specific activity are essential, while factors influencing weathering rates (Kashparov et al., 1999) such as particle size distribution, crystallographic structures, and oxidation states are necessary for long term ecosystem transfer (Salbu et al., 2001a).

In terms of impact and risk assessment, the bioavailability and uptake of particle-bound radionuclides has been ignored in comparison with those existing as ions or simple molecules. Also, there is lack or scarcity of information regarding weathering processes and remobilization of associated radionuclides in addition to biological impact that represent pathways relevant for particle contamination (Salbu, 2009a).

### *2.5.3. Importance of considering radioactive particles*

Radioactive particles are known to behave differently from the ionic species on which majority of risk and impact assessment models are based. As is often the case with areas contaminated by radioactive particles, failure to account for radioactive particles can lead to large uncertainties and significant errors in risk and impact assessment (Salbu, 2009a; Salbu, 2016). This is because particles can influence mobility and bioavailability of associated radionuclides. Therefore, particles associated with radiocesium will be important due to their long term persistence in the environment and high radiological hazards. It is therefore crucial to estimate the potential mobility and bioavailability of particle associated radiocesium in soil and sediments by way of speciation analysis. This work will be of particular importance to environmental and impact assessment, as well as disposal of nuclear wastes.

Consequently, a proper understanding of the chemical behavior of radiocesium forms the basis for sound long-term monitoring of Cs transport, proper management of land use, and radiation protection in the Fukushima area. It is known that the ecological significance of radioactive particles depend on the characteristics of the particles. Research has indicated that within an ecosystem, the speciation of radionuclides is related to sources and release scenarios, distance from the source, dispersion processes and deposition conditions (Lind et al., 2009; Salbu et al., 2001b). In the case of the Chernobyl accident, non-oxidized or seemingly reduced and inert U particles were released from U fuel during explosion and mechanical destruction of the UO<sub>2</sub> fuel under high temperature and pressure conditions without air, and deposited to the west of the reactor (Kashparov et al., 1999; Salbu, B, 2000; Salbu et al., 2001a; Salbu et al., 2015). A subsequent fire that occurred in the graphite moderator under oxidizing conditions at lower temperature and pressure resulted in the release of volatile fission products and oxidized U<sub>3</sub>O<sub>8</sub> fuel particles to the north, northeast and south of the plant (Kashparov et al., 2003; Lind, 2006). These latter oxidized particles were known to have at least 10 times higher weathering rates in comparison to the former reduced particles. The oxidized U particles were known to result in rapid ecosystem transfer of particle-associated radionuclides (like transfer of <sup>90</sup>Sr from soil to plants), while inert particles resulted in very slow ecosystem transfer (Salbu et al., 2001a).

## 2.6. Chemical, Physical and Environmental Properties of Cesium

### 2.6.1. Cesium

Cesium (Cs) is a silvery white soft and ductile metal that occurs both naturally and artificially, having about 40 known isotopes, more than any other chemical element (Gupta & Walther, 2017). It was discovered by Bunsen and Kirchhoff in 1860 at a Bavarian mineral spring (Avery, 1996). The stable  $^{133}\text{Cs}$  is the only naturally occurring cesium isotope, found in very low concentrations in some feldspars and micas (e.g. pollucite and rhodizite)(Comar, 1955; Patnaik, 2003).

Artificially derived Cs sources include nuclear reactor explosions, nuclear reactor operations and nuclear weapons tests. From the radiological point of view, seven significant isotopes of Cs are produced through the fission of various uranium, plutonium, and thorium, or the neutron bombardment of  $^{133}\text{Cs}$  or  $^{136}\text{Ba}$  (Dubchak, 2017; Longworth et al., 1998). A special mention is hereby made of  $^{137}\text{Cs}$ , which is a  $^{235}\text{U}$  fission product of high yield; and  $^{134}\text{Cs}$ , being an activation product. Table 1 provides a summary of the seven radioisotopes of Cs. Only three out of these radionuclides have relatively long half-lives (i.e.  $^{134}\text{Cs}$  ( $t_{1/2} = 2.1$  y),  $^{137}\text{Cs}$  ( $t_{1/2} = 30.17$  y) and  $^{135}\text{Cs}$  ( $t_{1/2} = 2.6 \times 10^6$  y)). These long-lived radionuclides of Cs decay by  $\beta$ -particle emission, although  $^{134}\text{Cs}$  can also undergo electron capture. Those of particular environmental importance include  $^{137}\text{Cs}$  and  $^{134}\text{Cs}$ . Due to the very low specific activity (except under nuclear explosion conditions),  $^{135}\text{Cs}$  and  $^{134}\text{Cs}$  can be of less concern. However,  $^{137}\text{Cs}$  is of particular environmental concern due to its long half-life, in addition to the release of an energetic  $\gamma$ -ray (with a  $t_{1/2} = 2.6$  min) from its decay product, (which is metastable barium) (Atwood, 2013). The strong  $\beta$ - and  $\gamma$ -radiation makes  $^{137}\text{Cs}$  both an internal and external hazard. In assessing the risk of radiocesium (mobility and bioavailability) in a given area, it is important to consider which Cs radioisotopes are present and the chemical form.

Table 1: Common cesium radioisotopes produced by nuclear fission and activation (Adapted from Atwood (2013))

Isotope	Mass	Half-life	Decay-type
$^{130}\text{Cs}$	129.90671	29.31 min	Electron capture to $^{130}\text{Xe}$ and $\beta^-$ to $^{130}\text{Ba}$
$^{131}\text{Cs}$	130.90546	9.69 days	Electron capture to $^{131}\text{Xe}$
$^{132}\text{Cs}$	131.906430	6.48 days	Electron capture to $^{132}\text{Xe}$ and $\beta^-$ to $^{132}\text{Ba}$
$^{134}\text{Cs}$	133.906714	2.065 years	Electron capture to $^{134}\text{Xe}$ and $\beta^-$ to $^{134}\text{Ba}$
$^{135}\text{Cs}$	134.905972	$2.3 \times 10^6$ years	B- to $^{135}\text{Ba}$
$^{136}\text{Cs}$	135.907307	13.16 days	B- to $^{136}\text{Ba}$
$^{137}\text{Cs}$	136.907085	30.17 years	B- to $^{137}\text{Ba}$

A special emphasis on  $^{137}\text{Cs}$  is hereby presented since it is the main Cs radioisotope considered in this work.  $^{137}\text{Cs}$  was discovered in the late 1930s by Seaborg and Melhase (Dubchak, 2017). The main characteristic properties include the following: long physical half-life,  $\beta$  and  $\gamma$  emitter; main emission  $\gamma$ -line is  $E_\gamma = 0.662$  MeV with quantum yield  $k_\gamma = 0.892$ ; maximum  $\beta$ -energy is  $E_{\beta\text{max}} = 1.172$  MeV; daughter product  $^{137}\text{Ba}$ . Figure 4 provides an overview of the decay scheme of  $^{137}\text{Cs}$  pointing towards its  $\gamma$  emission, as the main contributor to the overall level of external and internal exposure at contaminated areas (such as FEZ), in addition to the long term radiological impact.

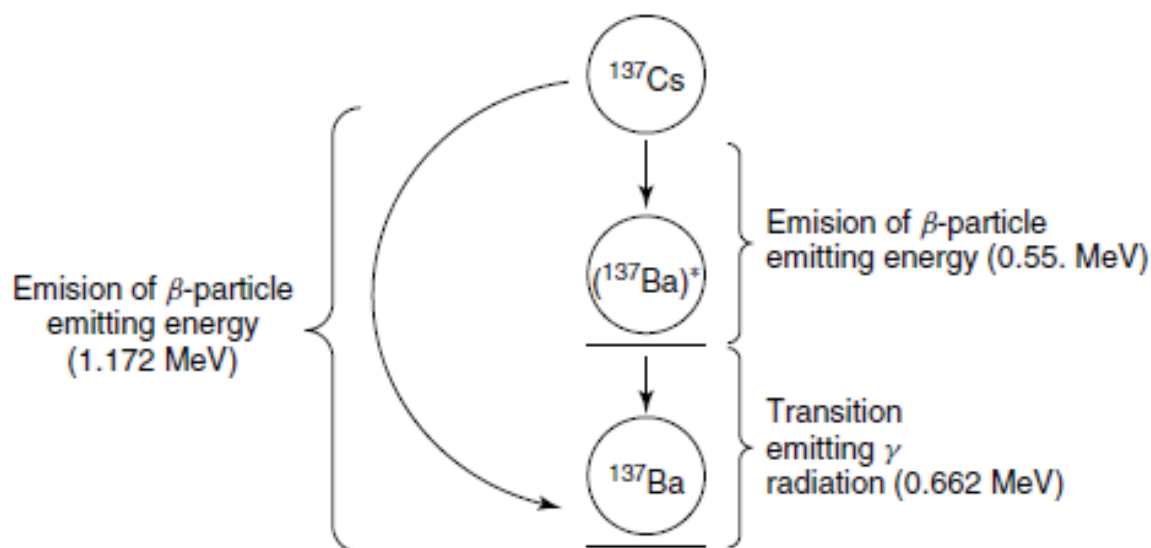


Figure 4: Simplified decay diagram of  $^{137}\text{Cs}$ . About 94% of Cs nuclei decay to an excited state of  $(^{137}\text{Ba})^*$  which subsequently decays by emitting  $\gamma$ -radiation. Adapted from Atwood (2013)

#### 2.6.2. Physical and chemical properties

Cesium (Cs) is classified as a Group IA alkali metal with atomic mass of  $132.91 \text{ g mol}^{-1}$  and an oxidation state of +1 (Atwood, 2013). Among the alkali metals in Group IA of the periodic table, Cs is considered the heaviest (having atomic number of 55), with the exception of francium, which is radioactive and occurs naturally only as part of the neptunium and actinium decay series (NCRP, 2006). Within this group, Cs is the most reactive and the most electropositive. Besides, it has the lowest boiling and melting points, highest vapor pressure, highest density, and lowest ionization potential. These properties make Cs far more reactive than the other members of the alkali metal group. When exposed to air, cesium metal ignites, producing a reddish violet flame, and forms a mixture of cesium oxides. Pure cesium reacts violently with water to form cesium hydroxide, the strongest base known, as well as hydrogen gas. The burning Cs can ignite the liberated hydrogen gas and produce an explosion.

Radiocesium emits ionizing radiation that can cause several adverse health effects on exposed populations, with several reports showing that fallout of nuclear accident are associated with radiological hazards. It is established that the high energy beta particles and gamma rays emitted from radiocesium can ionize molecules within human cells penetrated by the emissions (ATSDR, 2004). The possible results could be tissue damage and disruption of cellualr function.

External exposure to radiocesium and ingestion of radiocesium contaminated foods are considered the most important exposure routes. Other exposure routes of importance may include dermal exposure and inhalation. Depending on the absorbed dose, acute or repeated exposure of humans or animals to radiocesium may result in reduced male fertility, abnormal neurological development following exposure during critical stages of fetal development, and genotoxic effects such as increased frequencies of chromosomal aberrations, T-lymphocyte point mutations, dominant lethal mutations, and reciprocal translocations.

#### *2.6.3. Factors influencing cesium species in terrestrial and aquatic systems*

Radiocesium released into the environment tends to accumulate and reside primarily in soils and sediments (Whicker et al., 1990). This necessitates the study of radiocesium behaviour in soil and sediments, and their radioecological significance. It is believed that the behaviour of Cs in aquatic and terrestrial ecosystems are quite similar (NCRP, 2006). The fate of released radiocesium in the environment generally depends on the physical and chemical processes, and biological uptake. Radionuclides (including radiocesium) are known to have the same chemical properties as their stable elements, with little differences resulting from the difference in mass. However, these differences can be ignored in evaluation of radionuclide behaviour in terrestrial and aquatic systems (Nagy, 2012; Pentreath, 1988; Poinssot & Geckeis, 2012)

In soil and aqueous media cesium occurs as a free hydrated monovalent cation ( $\text{Cs}^+$ ), due to the high solubility of cesium salts (chemically present as  $\text{CsI}$ ,  $\text{CsOH}$ , and  $\text{Cs}_2\text{CO}_3$ ) and the affinity of clays to retain cesium cations in the interlayer spaces (Atwood, 2013; Huheey et al., 2006). The fixation ability of clays and leaching from the root zone in soils reduces Cs bioavailability with time. Cesium has chemical properties similar to potassium and rubidium, having little or no tendency to form soluble complexes in the soil.

Radiocesium deposited on the surface of the soil or water as fallout or introduced otherwise is prone to both vertical and horizontal transfer. Besides, the movement through soil and sediment can either be vertical or horizontal. To a large extent, terrestrial transport is determined by interrelated factors such as: (1) climate and weather, (2) terrain and topography, (3) soil type and characteristics, and (4) vegetation and animal life (Kathren, 1984). On the other hand, several mechanisms also account for the removal of radiocesium from aquatic systems (surface water)

into sediments. These include geometry (i.e. size, shape, depth), and temperature profile of the water body, weather, salinity, and state; whether the water is impounded (like lakes and ponds) or free flowing (like rivers). Other factors include uptake, concentration and excretion by biota. A summary of the factors is provided in Table 2.

*Table 2: Factors influencing aquatic transport (Kathren (1984))*

Physical factors	Chemical Factors	Biological Factors
Precipitation (e.g. rainfall, snow)	Dissolution of solids	Uptake and concentration in biota
pH	Precipitation	Excretion
Gravitational settling	Oxidation-reduction reactions	Transport by mobile species
Resuspension	Ion exchange	
Wind	Sorption	
Thermal gradient	Chemical combination	
Radioactive decay	Photochemical reactions	
Groundwater influence		

For terrestrial ecosystems, soil plays a particularly important role, because it is the available fraction of  $^{137}\text{Cs}$  in soil that determines biological uptake, while the strength of its binding to soil particles determine transport (NCRP, 2006). Generally, a high degree of mobility and bioavailability of radiocesium is dictated by the uncomplexed  $\text{Cs}^+$  ion (Avery, 1996), as  $\text{Cs}^+$  exhibits little tendency to form aqueous complexes in the soil/water environment. However, the partitioning of  $\text{Cs}^+$  between abiotic (i.e. soils, sediments, water) and biotic (e.g. microorganisms, plant, and animals) components of terrestrial and aquatic ecosystems is associated with some level of complexity, due to a number of factors such as organic and inorganic mineral content of the solid substrates, and the abundance of other monovalent cations.

Sorption by soil or sediment is an important mechanism by which radiocesium may be removed from fluid medium like water. Sorption of cesium to soil or sediments is highly dependent on the

mineralogy of the soil or sediment (NCRP, 2006). A common way of describing the strength of binding or partitioning between soils or sediments and the aqueous phase (i.e. sorption) is by the concept of partition or distribution coefficient ( $K_d$ ). The distribution coefficient ( $K_d$ ) is expressed as the concentration of contaminant in the soil or sediment divided by the concentration in the water at equilibrium, and having a unit of  $\text{mLg}^{-1}$ . For instance, a relatively high  $K_d$  value ( $>100 \text{ mLg}^{-1}$ ) implies strong binding to soil particles, and slow movement in soil relative to water.

In a contaminated environment, direct biological uptake and accumulation of  $\text{Cs}^+$  is known to readily occur in primary producers and lower organisms (e.g. microorganisms and plants), while the consumption of contaminated foodstuffs is the predominant means by which  $\text{Cs}^+$  accumulates in higher animals (Avery, 1996). The ease with which  $\text{Cs}^+$  is taken up by plants, animals, and humans is due to its chemical similarity with  $\text{K}^+$  causing internal exposure. Additionally, direct inhalation or absorption of  $\text{Cs}^+$  from the environment may also occur through resuspension.

Uptake by plants is the dominant pathway by which radiocesium migrate from soil to humans (Gupta & Walther, 2017). Reports of radiocesium accumulation into terrestrial plants such as tea, rice, sunflower, and tomato has been documented. Two principal mechanisms account for plant accumulation of radiocesium: (1) direct deposition from the atmosphere and (2) root uptake. Aerial deposition results in accumulating Cs in the leaves of plants, and this may disturb the basic physiological functions of plants, as evidenced by several physiological experiments. Root uptake of radiocesium is known to occur via soil solution, hence, the higher the concentration of radiocesium in the soil solution, the greater is its concentration in a plant. However, the concentration of radiocesium in the soil solution can vary significantly, and this depends to a large extent on the sorption properties (e.g. CEC, FES capacity, fixation ability) and on the ion composition of the soil solution (i.e. concentration of competitive ions like  $\text{NH}_4^+$  and  $\text{K}^+$ ) (Konoplev et al., 1999; Konoplev et al., 2000; Rigol et al., 2002).

Soil pH also exerts some control over the mobility and solubility of radiocesium in soils. It is known that bioavailability increase with the reduction of soil pH through cationic exchange,

since  $\text{Cs}^+$  may be replaced by  $\text{H}^+$  (Bakken & Olsen, 1990). Acidic conditions are known to favour biological availability of  $^{137}\text{Cs}$  in soil, while uptake by plants and subsequent transfers to higher trophic levels is suppressed by high concentrations of potassium (NCRP, 2006). Heinrich (1992), have demonstrated the pH dependence of  $\text{Cs}^+$  in acidic soil with a high concentration of humus, and the results showed an increased uptake of  $\text{Cs}^+$  by mushrooms. A general conclusion drawn on the biogeochemical behaviour of cesium in terrestrial ecosystems is that  $\text{Cs}^+$  demonstrates a low mobility in the soil profile (Rosén et al., 1999), but, there is a relatively high movability in biological systems (Dubchak, 2017). Other authors (Huang et al., 2016; Yoshida & Muramatsu, 1994; Yoshida et al., 1994) have also shown that, the rate of  $^{137}\text{Cs}$  vertical migration is slow in nutrient-poor forest soils, however, a high bioavailability was encountered, especially in fungal species.

Generally, it is believed that radiocaesium isotopes deposited from fallouts are mainly retained in the upper 10–15 cm of the soil profile due to low rate of vertical migration, which is about several millimeters per year (Mahara, 1993). Depending on the bioavailability, among other factors, such localization of radiocesium could be hazardous, since the upper layers of the soil are extensively accessed by fungal mycelium, plant roots and other soil microorganisms (Thiry & Myttenaere, 1993). It is worth noting that there is a difference between the distribution pattern of radiocesium isotopes and that of the natural stable  $^{133}\text{Cs}$ , which is relatively distributed uniformly through the different soil profiles (Bakken & Olsen, 1990). Meanwhile, microbe-associated  $^{137}\text{Cs}$  has been estimated to represent about 1–56% of the total content in the upper organic layers of forest soils (Brückmann & Wolters, 1994). It has been observed that absorption of  $^{137}\text{Cs}$  can approach 100 % in lichens and mosses, with a much longer retention time (NCRP, 2006). This indicates that at a particular contaminated location, radiocesium can recirculate continuously in biological systems for several years following a pulse of contamination. Nevertheless, the time-scale of  $^{137}\text{Cs}$  retention in higher organisms and environmental objects in relation to the biological and environmental half-lives (Table 3), indicates that accumulation of  $^{137}\text{Cs}$  does not last indefinitely.

Table 3: Retention time-scale indicating the biological and environmental half-lives of  $^{137}\text{Cs}$  in organisms and environmental objects. Adapted from Dubchak (2017)

	Organism/Environment	Half-life
<b>Biological</b>	Moss	4–5 years
	Lichen	5–8 years
	Grass	14 days
	Plant leaf surface	14 days
	Hen	1–5 days
	Cow	3 days
	Fish	70–300 days
	Child	57 days
	Woman	84 days
	Man	105 days
<b>Environmental</b>	Lake	2–7 years
	River	1–4 years
	Airborne dust	270 days

There are several routes by which humans can be exposed to  $^{137}\text{Cs}$  externally and/or internally following a release to the atmosphere (Figure 5). Considering the aquatic ecosystem, there are certain pathways of concern for  $^{137}\text{Cs}$ . First is the direct external radiation via freshwater sediments, which is of primary concern for individuals who reside or spend recreational time on the shores of these (Kathren, 1984). On the contrary, the burial of  $^{137}\text{Cs}$  through accumulation of less-contaminated sediments over time can result in the removal of  $^{137}\text{Cs}$  from interactions with biota, surface sediments, or overlying water (NCRP, 2006). Other pathways of concern originates from the direct use of water for drinking and irrigation purposes, as well as the pathway through freshwater fish, especially bottom feeders and dwellers. Although the biological half-life of Cs is relatively short, Cs is known to be efficiently absorbed from the gut of animals for transport to muscle and milk.

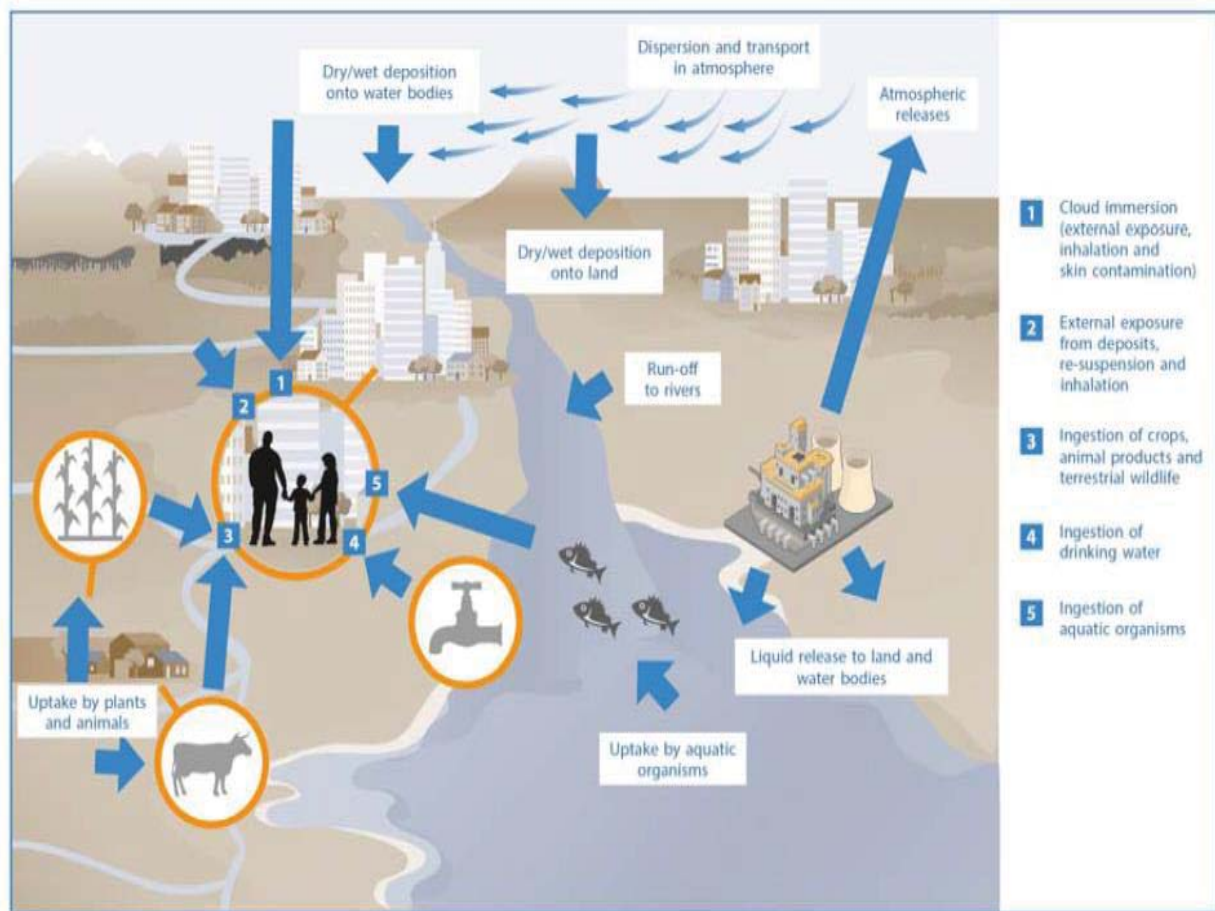


Figure 5: Pathways of exposure following the release of  $^{137}\text{Cs}$  to the environment. Adapted from UNSCEAR (2014)

Pathways through plants can begin with pasture grass consumed by grazing animals and through milk or meat. Since  $^{137}\text{Cs}$  is somewhat uniformly distributed throughout all portions of plant parts, and does not necessarily concentrate only in the edible portions, coupled with the poor absorption by some plants, the overall pathway through plant foods may be relatively unimportant, except for grains (Kathren, 1984).

### **3. MATERIALS AND METHODS**

#### **3.1. Site and Sample Description**

In this study, archived soil and sediment samples originating from the 30 km Fukushima Exclusion Zone (FEZ), Japan were used. The samples were collected by NMBU staff during a field trip to Fukushima, Japan in September 2016. The sites studied were within 11 km of the damaged FDNPP reactors. The sampling locations where cores were obtained are shown in Figure 6 with their respective site description in Table 4. The yellow line in the map represent the direction of the plume.

Beside sampling for soil and sediments, litter samples were also collected during the field work. Samples were taken at various distances and different directions from the epicenter of the accident (FDNPP). Samples were collected predominantly from downwind, and those areas suspected to have high activities with the help of handheld gamma dosimeters and windrose data. Other locations were selected close to the point of predicted maximum ground concentrations and areas which may be potentially contaminated within the plume and mixing zones, as well as areas accumulated from downwind or from surface run off. Other samples were taken further from the potential point of release. Transects were laid, in addition to soil and sediment profiles at some sites. Layers of soil samples were taken with 0–5cm capacity and some to a depth of 10 cm.

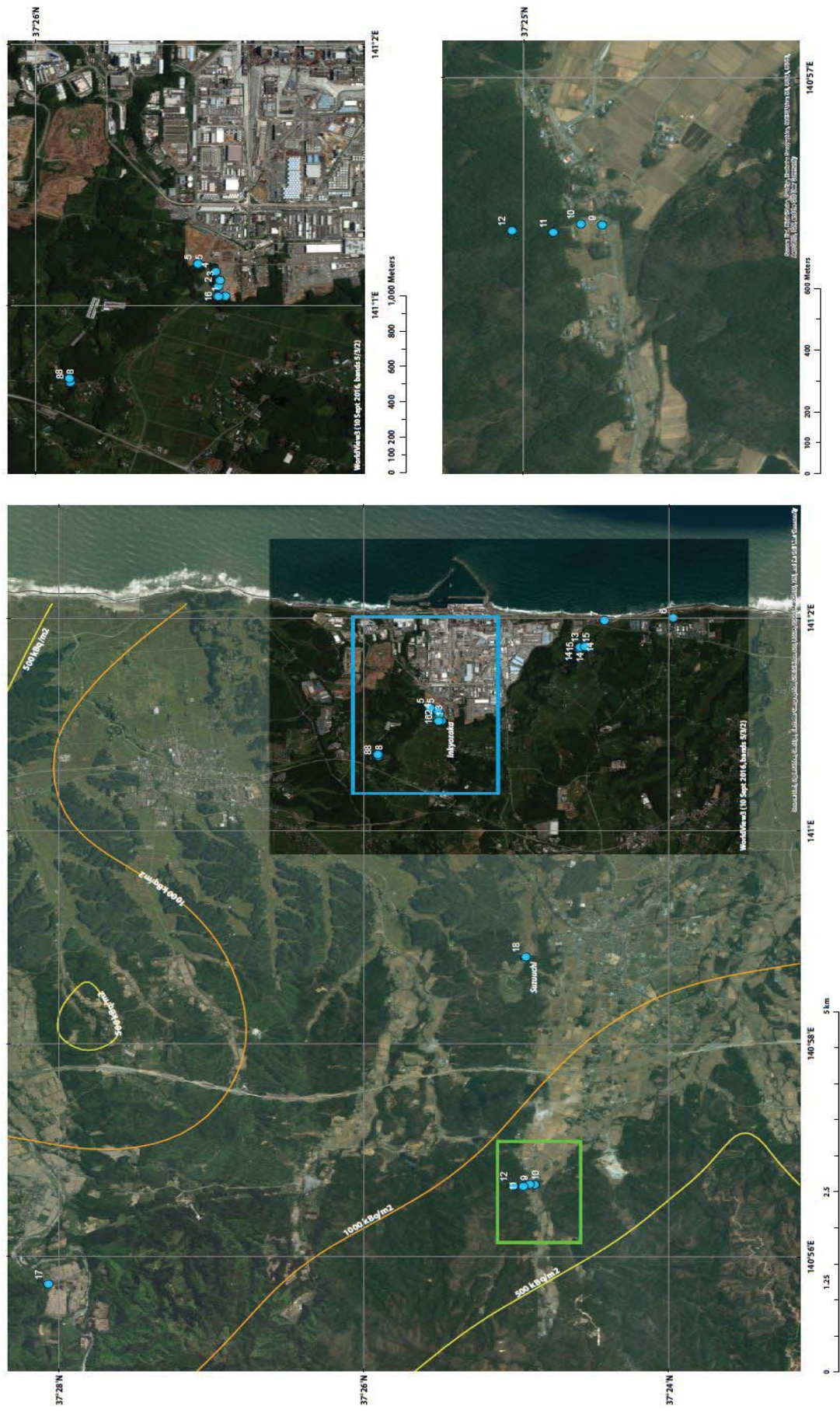


Table 4: Information regarding samples and sampling location

Site #	Sample type	Sampling date	Coordinates			Distance (m)	Heading to reactor	WindRose	Site description
			Longitude	Latitude					
1	soil, 0-3 cm	25.09.2016	141°01'0.11" E	37° 25' 29.4" N		1451.78	-17.51	WNW	Northwest of reactor, transect between Inkyozaka pond and FDNPP
1	litter	25.09.2016	141°01'0.11" E	37° 25' 29.4" N		1451.78	-17.51	WNW	Northwest of reactor, transect between Inkyozaka pond and FDNPP
4	soil, 0-6 cm	25.09.2016	141° 0107.67" E	37° 25' 1.01" N		1337.35	-21.27	WNW	Northwest of reactor, transect between Inkyozaka pond and FDNPP
4	litter	25.09.2016	141° 01' 07.67" E	37° 25' 1.01" N		1337.35	-21.27	WNW	Northwest of reactor, transect between Inkyozaka pond and FDNPP
5	soil, 0-6 cm	25.09.2016	141° 01' 09.53" E	37° 25' 3.77" N		1331.49	-25.46	WNW	Northwest of reactor, transect between Inkyozaka pond and FDNPP
6	soil, 0-3 cm	27.09.2016	141° 02' 0.31" E	37° 23' 8.32" N		2370.92	91.13	SSE	South of reactor, forest by the sea
7	soil/gravel/s and, 0-5 cm	27.09.2016	141° 41' 59.89" E	37° 24' 5.25" N		1540.55	90.35	SSE	South of reactor, concrete platform next to fish factory by the sea
7	soil/gravel/s and, 5-10 cm	27.09.2016	141° 41' 59.89" E	37° 24' 5.25" N		1540.55	90.35	SSE	South of reactor, concrete platform next to fish factory by the sea
8	soil from run-off	25.09.2016	141° 00' 43" E	37° 25' 54" N		1451.78	-17.51	WNW	Northwest of reactor, ditch (concrete) outside a house
9	soil/gravel, 0-2.5 cm	24.09.2016	140° 56' 20" E	37° 24' 52" N		7842.19	5.06	WSW	West of reactor, road into forest, near graveyard
10	soil, 0-6 cm	24.09.2016	140° 56' 40" E	37° 24' 55" N		7833.93	4.63	WSW	West of reactor, road into forest, near graveyard
13	soil	23.09.2016	141° 01' 44" E	37° 24' 33" N		1348.87	74.77	SSW	Southwest of reactor, outside a house
14	soil, top layer	23.09.2016	141° 01' 43" E	37° 24' 3.18" N		1290.96	72.92	SSW	Southwest of reactor, Okuma
16A	soil, 0-5 cm	23.09.2016	141° 01' 2.07" E	37° 25' 0.58" N		1463.89	-18.83	WNW	Northwest of reactor, pond between forest and FDNPP
16B	surface sediment	23.09.2016	141° 01' 2.07" E	37° 25' 0.58" N		1463.89	-18.83	WNW	Northwest of reactor, pond between forest and FDNPP
17	soil, 0-20 cm	25.09.2016	140° 54' 24" E	37° 27' 56" N		10560.67	-29.53	WNW	Northwest of reactor, by Omaru shrine
18	surface sediment	23.09.2016	140° 58' 49.14" E	37° 24' 56.2" N		4689.75	7.19	WSW	West of reactor, fish pond

In terms of sampling, handling, treatment, characterization and analysis of soils, sediments and vegetation, utmost care was taken to avoid cross contamination of the samples, and to obtain reliable experimental results. This was not only limited to ensuring sampling integrity, but also cautions were taken in using clean independent containers at all times, in addition to avoiding the introduction of foreign materials or contamination from other sources. It was also ensured that the original distribution of radiocesium at the time of sampling was preserved.

### **3.2. Soil and Sediment Characterization**

The characteristics of soil and sediments are likely to influence the speciation of radionuclides, and can contribute to confounding factors when not adequately determined. In addition, undertaking a good characterization helps to avoid false assumptions. Characterization of  $^{137}\text{Cs}$  was performed at a variety of locations in a FEZ. This provides the distribution patterns of  $^{137}\text{Cs}$  with the aim of identifying areas of potentially enhanced exposures as a result of the FDNPP accident. Standard procedures for determining soil and sediment characteristics were followed.

#### *3.2.1. Sample preparation*

Sample preparation procedures are of great importance for obtaining reliable experimental results. The major goal is to prepare a sample in such a way that the original elemental distribution at the time of sampling is preserved and that the introduction of foreign elements is avoided. Soil and sediment samples were homogenized wet, freeze dried and then sieved, and that the water content was determined by mass difference before and after freeze drying. The freeze dried fractions were then sieved to  $< 2$  mm, and bigger than  $> 2$  mm was discarded. Subsamples were then taken from the  $< 2$  mm fractions for the characterisation. The samples were stored at  $4\text{ }^{\circ}\text{C}$  from sampling day until the day of analysis to limit biological activity.

#### *3.2.2. pH measurement*

The pH of samples were measured as a part of the sequential extraction procedure using a pH meter (WTW InoLab® pH 720). The procedure involves calibration of the pH meter, followed by the addition of MilliQ- water (reverse osmosis and purified through a MilliQ-filter) to the soil or sediment samples in the ratio of 1g:20 mL representing volumes of solid sample:water left to equilibrate overnight and the pH measured.

### *3.2.3. Grain size distribution*

Organic matter in solid samples (soil or sediment) was removed by the addition of H<sub>2</sub>O<sub>2</sub> while heating until no more reaction. This was followed by wet sieving through 0.06 mm to remove the sand fraction. All the filtrate (water) was collected to do sedimentation of the silt fraction as a function of distance and time (based on Stoke's law). According to Stokes' law, the amount that a particle sinks depends upon the density of the particle. This means denser (larger) particles sink more than less dense (smaller) particles when suspended in a liquid. The clay fraction remained in the water. All fractions were dried at 105°C, and percentage distribution was calculated from the dry weights of all fractions.

### *3.2.4. Determination of organic matter content*

Samples were dried overnight at 105 °C, and the warm samples were put in a dessicator prior to weighing. Then the sample were ashed in a stepwise procedure up to 550 °C for 20 hours (24 hours in total). The percentage loss of ignition (LoI) is equal to the organic matter.

## **3.3. Sequential extraction**

Sequential extractions of contaminated soils and sediments is a widely applied method used to study reversible or irreversible interactions of radionuclides with solid phases, using reagents to differentiate between binding mechanisms (Oughton et al., 1992; Skipperud et al., 2000b; Skipperud et al., 2009; Skipperud & Salbu, 2015). The study of the different forms of cesium found in soil and sediments can allow for the evaluation ability of long-lived radionuclides (like <sup>137</sup>Cs) to migrate in terrestrial and aquatic ecosystems. Subsequently, the variability in assessing environment risks will be reduced considerably when the total soil concentration of radiocesium is replaced by its bioavailable fraction. Another fact of importance is that within an aquatic system, chemical exchange between water and bottom sediments could occur leading to the secondary source of water contamination by radiocesium.

The sequential extraction method used in this work was based on the protocol proposed by Tessier et al. (1979) and modified by Skipperud and Salbu (2015). The experiments were performed in the Isotope Laboratory (Center of Environmental Radioactivity) at the Norwegian University of Life Sciences. The procedure was based on using fresh soil or sediment samples, having a sample:solution ratio of 1 g:10 mL (Kennedy et al., 1997). For sequential extractions, 2

grams of sample were weighed in triplicates into acid-washed centrifuge tubes. Samples were selected based on (i) low organic matter content in order to avoid explosion when reacting with  $\text{H}_2\text{O}_2$ , (ii) varying soil chemical properties and (iii) wide range of activities. A total of seven samples ( $n=7$ ) were selected for the sequential extraction, and this is made up of soils from sites #7, #8, #10, #13, and #16 ( $n=5$ ) and pond sediments from sites #16 and #18 ( $n=2$ ). The pH of the samples were measured prior to extraction. The experiment was run in three batches over three weeks with due consideration to the centrifuge, which had capacity for eight centrifuge tubes. For Week 1, samples ran include triplicates for #16A and #10, in addition to two blanks. Week 2 samples were triplicates of #18 and #16B, and two from #7. In the final week (Week 3), the samples involved triplicates from #8, and #13, in addition to one blank and one sample from #7. The extraction was conducted in a fume hood according to a sequence presented below.

**F1.** MilliQ-water (20 mL) was added to the solid sample in the centrifuge tube. The sample was swirled to mix, and placed on a roller mixer (Stuart<sup>TM</sup> roller mixer SRT6) for 1 hour at room temperature. The sample was centrifuged at 10 000 rpm (using a BeckmanCoulter<sup>TM</sup> Allegra 64R Centrifuge) for 25 minutes. After centrifugation, the solution was filtrated through a 110 mm round filter blue band filter in a funnel with the aid of disposable plastic pipette. The supernatant was collected in 20 mL polyethylene vials. This fraction is defined as the water soluble species.

**F2.** 20 ml of 1M  $\text{NH}_4\text{Ac}$  (adjusted to pH of sediment or soil) was added to the residue from F1 and the sample was placed on the roller mixer for 2 hours at room temperature. It was then centrifuged at 10 000 rpm for 25 minutes followed by filtration. The supernatant was collected in 20 mL polyethylene vials. This fraction reflects species associated with solids via physical sorption mechanisms, which is mainly exchangeable species. It should be noted that this step was skipped for samples with pH below 5.

**F3.** 20 mL 1M  $\text{NH}_4\text{Ac}$  (pH 5) was added to the residue from F2. The sample was placed on a roller mixer for 2 hours at room temperature. Followed by centrifugation at 10 000 rpm for 25 minutes. The supernatant was collected in 20 mL polyethylene vial. The sample was then washed with 10 mL MilliQ-water followed by centrifugation for 15 minutes and filtrated. The

supernatant of this washing step was collected in 20 mL polyethylene vial. The fraction (combined filtered supernatants of this step) reflects species associated with carbonates.

**F4.** 20 mL 0.04 M  $\text{NH}_2\text{OH}\cdot\text{HCl}$  in 25% (v/v) HAc (adjusted to pH 3) was added to the residue from F3. The sample was heated for 6 hours in a water bath (GRL 1092 shaking water bath) at 80°C. It was then centrifuged for 25 minutes and then filtered. The supernatant was collected in 20 mL polyethylene vial. The sample was washed with 10 mL MilliQ-water followed by centrifugation for 15 minutes and then filtrated. The supernatant of this washing step was collected in 20 mL polyethylene vial. The fraction (combined filtered supernatants) reflects species associated with solids via chemical sorption mechanisms, which are released into the extraction solution with weak reducing agent. The species here are mainly those bound to Fe/Mn oxides.

**F5.** 15 mL  $\text{H}_2\text{O}_2$  (30%) adjusted to pH 2 with concentrated  $\text{HNO}_3$  was added to the residue from F4. The sample was warmed in a water bath at 80°C for 5.5 hours. Then 5 mL 3.2 M  $\text{NH}_4\text{Ac}$  in 20% (v/v)  $\text{HNO}_3$  was added to the mixture in the centrifuge tube. It was placed on a roller mixer for 0.5 hours followed by centrifugation at 10 000 rpm for 25 minutes. The supernatant of was collected in 20 mL polyethylene vial. The sample was washed with 10 mL MilliQ-water before being centrifuged for 15 minutes followed by filtration. The supernatant of the washing step was collected in 20 mL polyethylene vial. The fraction (combined filtered supernatants) reflects species associated to solids that can be released with an oxidising agent (i.e. primarily, organic matter or uranium oxides).

**F6.** 20 mL 7M  $\text{HNO}_3$  was added to the residue from F5. The sample was heated in a water bath at 80°C for 6 hours with swirling periodically, before being centrifuged at 10 000 rpm for 25 minutes. The sample was washed with 10 mL MilliQ-water before being centrifuged for 15 minutes and filtered. The combined filtered supernatants relects the acid dissovable fraction

**Rsd.** Residue and filter were dried and transferred to a vial. This fraction is considered as inert or insoluble fraction. The experimental setup is shown in Figure 7.

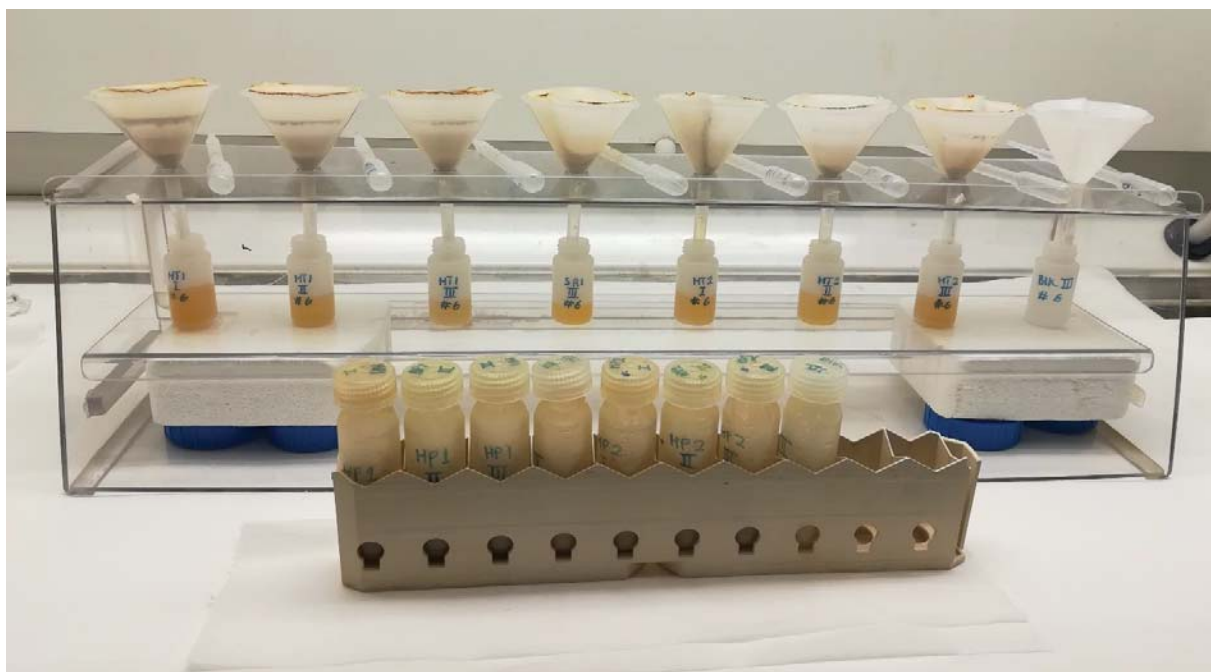


Figure 7: Experimental setup for the sequential extraction; plastic pipette beside funnels with inserted filters, placed in a funnel holder over sample vials, and centrifuge tubes in a rack.

Table 5 summarises the six extraction steps performed sequentially. All supernatants (extracts) and residue were measured on the gamma spectrometer with a NaI-detector (Wizard 3" 1480 Automatic Gamma Counter, Perkin Elmer Life Sciences). The data used for evaluation was the corrected counts per minute (ccpm).

The total extractable  $^{137}\text{Cs}$  recovered in the first three steps of the procedure (F1+F2+F3) represent the mobile  $^{137}\text{Cs}$  fractions in soils and sediments. These are considered to be reversibly bound in soils and sediments via physical and electrostatic sorption.

Table 5: Summary of sequential extraction procedure carried out in the laboratory

Fraction	Main associated species	Extraction reagent	Temperature	Contact time, hr
<b>F1</b>	Water-soluble	H <sub>2</sub> O	RT	1
<b>F2</b>	Exchangeable	1M NH <sub>4</sub> Ac - pH 7	RT	2
<b>F3</b>	Carbonates	1M NH <sub>4</sub> Ac - pH 5	RT	2
<b>F4</b>	Easily reduced compounds (Fe/Mn oxides)	0.04M NH <sub>2</sub> OH·HCl in 25% Acetic acid (pH~ 3)	80°C	6
<b>F5</b>	Oxidized Compounds (Organic material or Uranium oxides)	H <sub>2</sub> O <sub>2</sub> 30% (pH~2) (15 ml)	80°C	5.5
		3.2M NH <sub>4</sub> Ac (5 ml)	RT	0.5
<b>F6</b>	Acid dissolvable	7M HNO <sub>3</sub>	80°C	6
<b>Rsd</b>	Inert			

### 3.4. Leaching with 0.16 M HCl

Laboratory-based (in vitro) extraction procedures have been developed by toxicologists and other researchers to mimic biological ‘extraction’ using simulated digestive fluids (Ehlers & Luthy, 2003; Oomen et al., 2003; Ruby et al., 1999). By using standard analytical techniques, dissolved trace elements in the simulated biological fluid are then measured. The result is called the ‘bioaccessible’ fraction. This is the fraction that is ‘accessible’ for absorption into the bloodstream if ingested .

An important issue for consideration from a contaminated land health risk assessment perspective is the chemical forms that are extracted when soils containing trace elements are exposed to the leaching conditions in the human digestive system (Council, 2003). From the foregoing, the chemical form of a trace element that dissolve in digestive fluids can be absorbed

through the linings of stomach and intestines, enter the bloodstream and can be transported to different parts of the body.

Some researchers (Luthy et al., 2004; Williams et al., 1998) have investigated bioavailability to humans using animals that are physiologically similar to humans, since some animals are expected to take up contaminants in much the same way as humans do. However, efforts to reduce the need for animal testing for ethical and humane reasons, beside the high cost and longer time involved, have made using simulated stomach juice a preferred option for site-specific health risk assessment. This has resulted in the concept of bioaccessibility. Bioaccessibility of a trace element is the proportion of that element that can be extracted under simulated digestive conditions, while bioavailability is the proportion of that element that is absorbed from soil in the digestive system into the body. In a nutshell, bioavailability can be determined through bioaccessibility tests.

Generally, estimation of bioavailability is usually achieved by bioaccessibility assays using in vitro leaching techniques with synthetic agents analogous to digestive fluids (Golder Associates, 2016). This approach has inherent limitations due to: (1) the fact that synthetic agents cannot contain all the fluids (biotic) available in the stomach of interest, and (2) several mechanisms may control bioavailability of elements apart from dissolution (Voutsas & Samara, 2002). Notwithstanding, a validated in vitro leaching method can be a useful replacement for a more labour and capital-intensive site-specific animal models.

In this work, laboratory tests were carried out to extract a 'similar' proportion of  $^{137}\text{Cs}$  from soils and sediments as it would be absorbed by humans or animals upon ingesting contaminated soil or sediment from the area under consideration. About 0.5 g aliquot of contaminated soil or sediment sample was transferred to acid-washed centrifuge tubes and extracted with 20 mL of simulated human gastrointestinal (GI) tract fluid (i.e. 0.16 M HCl secretion of the digestive tract (White et al., 1968.)) for 65 hours. The 65 hour extraction time was chosen to mimic the transit time of a contaminated particle through the intestines (Darley et al., 2003) in order to evaluate the dissolution and absorption of particle associated  $^{137}\text{Cs}$  as a link to potential bioavailability and extraction kinetics.

### 3.5. Gamma measurements

Cesium emits both beta and gamma radiation, but only gamma radiation ( $\gamma$ ) is described in this work, since it was the only radiation type measured in the soils and sediments during the field and laboratory measurements, due to the ease of measurement. Considering that the samples were taken in the year 2016, (i.e. 5 years after the FDNPP accident had occurred), more than 80% of  $^{134}\text{Cs}$  is expected to have decayed (Dubchak, 2017). So,  $^{137}\text{Cs}$  becomes the main contributor to soil, sediment and vegetation contamination, as well as, to the population exposure in the heavily contaminated FEZ.

Gamma spectrometry allows for both qualitative and quantitative determination of gamma emitting radionuclides (like radiocesium) directly in the original samples by using detectors based on scintillation or semi-conductor principles. Two detectors of choice are sodium iodide (NaI) and germanium (Ge). While NaI-detectors consist of a cylindrical NaI crystal, Ge-detectors consists of a semiconductor material that interact with gamma radiation. Another important difference is that NaI-detectors provide better counting efficiency, while Ge-detectors provide better energy-resolution.

Samples were measured using gamma-ray analyzers with NaI-detector (PerkinElmer Wizard2<sup>®</sup> 2480 Automatic Gamma Counter) and two Ge-detectors (Ortec HPGe coaxial detector and Canberra GL 2020R LEGe detector, equipped with Ortec GammaVision software). The NaI-detector was the preferred choice due to the magnitude of samples assembled for measurement (especially, for extracts obtained from sequential extraction).

The content of  $^{137}\text{Cs}$  in all samples was determined with the Na-I detector (Figure 8) with a LoQ for the Cs-137 measurement (Cs-137 assay): being 11 DPM, calculated with the standard deviation of the background ( $\text{LoQ} = 14.1\sigma_B$ ). The efficiency of the Cs-137 measurement in the Cs-137/Cs-134 assay gave an average efficiency of 20,08%  $\pm$  0,04% (n=3). This was based on measurement of the high activity standard of Cs-137 (8970 Bq). The efficiency for Cs-137 in the Cs-137 assay was 19,98%  $\pm$  0,04%. So in general, 20% efficiency for Cs-137 was obtained when measured in the Cs-window as set in the Isotope library.

Samples with relatively high and low activities were counted for 1 hour and 2 hours respectively providing a precision of ca.  $\pm 10\%$  at the 95% level of confidence. The counting time was sufficient to obtain an acceptable analytical precision at  $2\sigma$  ( $< 10\%$ ). The effect of counting time on counting uncertainty was determined for different levels of activity Table 1A. It was established that increasing the counting times could not result in improving the uncertainty of the measurements (see Figure 9). For activities between 60 and 500 DPM (Figure 9a), the counting uncertainty decreased with increasing activities ( $\sim 10\%$  at 450 DPM) but was not improved with higher counting time (i.e., 1, 2 and 4 h). At the lowest activities ( $< 60$  DPM), the counting uncertainty decreased with counting time but was still relatively high even after 4 hours ( $\sim 50\%$ ). Similar trend was observed at activities between 500 and 10000 DPM (Figure 9b).



*Figure 8: Gamma measurements on NaI detector (PerkinElmer Wizard2® 2480 Automatic Gamma Counter)*

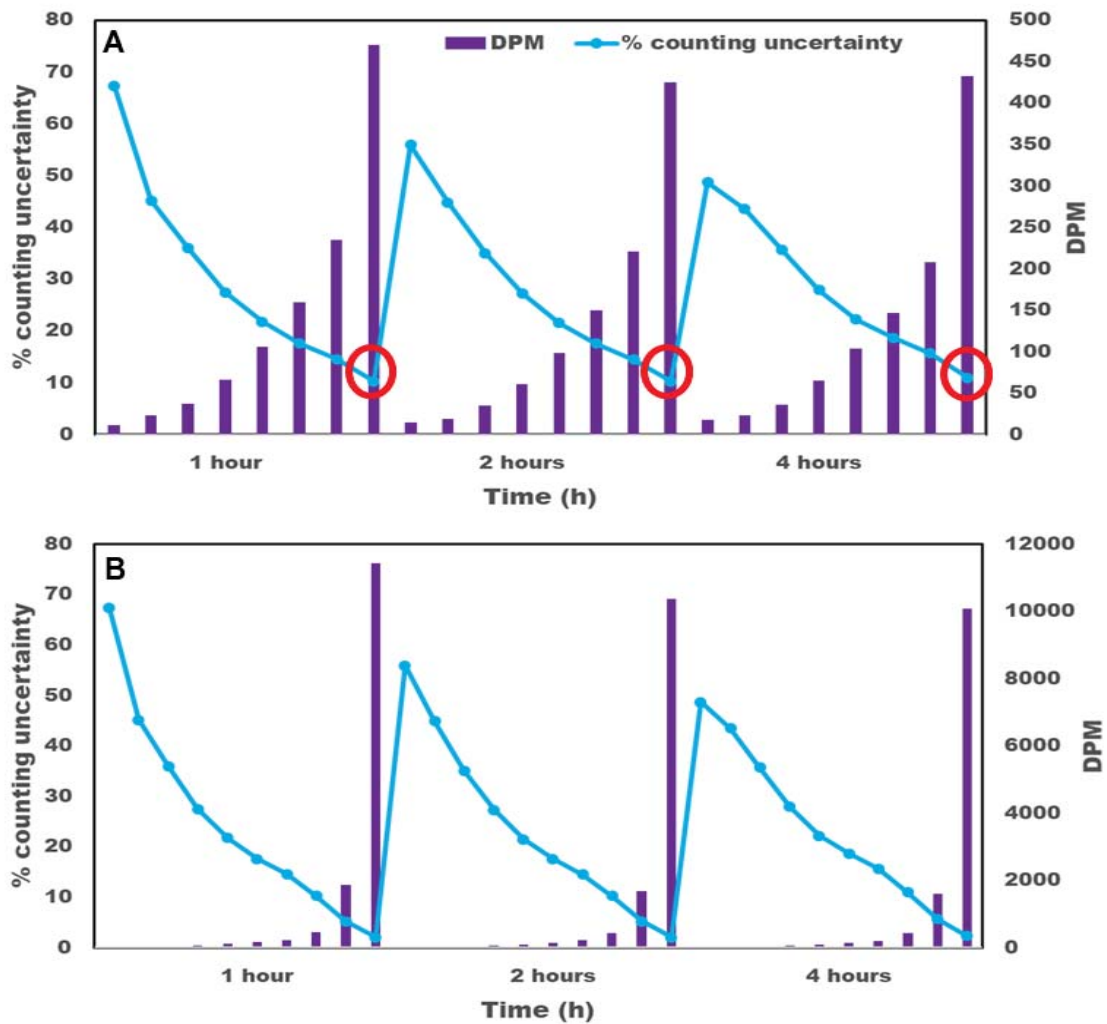


Figure 9: Effect of counting time on counting uncertainty: (a) activities <500DPM (b) >1000DPM

### 3.5.1. Interaction of gamma rays with matter

A brief background of how gamma rays interact with matter is hereby provided. Gamma measurement can be achieved through the detection of gamma rays (or photons) without the need for chemical separations. As a result of nuclear instability, these photons (particles that are emitted from the atomic nuclei) are capable of dislodging electrons from atoms and molecules. There are three types of interactive processes by which gamma rays (photons) can be absorbed or scattered by matter. These processes include (1) photoelectric effect, (2) Compton scattering, and (3) pair production. All the three interaction processes can result in the attenuation of the photon beam as it passes through matter. With these interactions, the material encountered may act as an

absorber of the signal. The interaction of gamma rays (photons) with either the NaI or Ge crystal produces electric signals that corresponds to the energy of the incoming photons (IAEA, 2014). During measurements, the electric signals are amplified and transmitted to a multi-channel analyzer (MCA). Then, a gamma energy spectrum, characteristic of the gamma-emitting nuclides will be produced as result of the three effects (i.e. Photoelectric, Compton and Pair production effects). The main characteristic of a photoelectric effect is the presence of high resolution peaks (called full energy peaks) that is associated with the gamma rays emitted by the radionuclides. Compton effect is characterized by a continuum due to the interaction of the gamma rays with electrons of the atom. Photoelectric effect is associated with the conversion of the net peak area (counts per second) of the nuclide of interest into activity (Bq kg<sup>-1</sup>). With an appropriate software package, the overall collected spectral data can then be processed.

### 3.6. Intercomparison of methods

Concentration of <sup>137</sup>Cs in some selected samples (reflecting a range between low and high activities) were measured on both NaI and Ge detectors as quality control. The two instruments showed comparable results ( $R^2 = 0.9989$ ) as shown in Figure 10. The uncertainty for the Na-I detector analysis given as relative standard deviation was less than 10 %, showing a good precision of the measurements, while that of the Ge-detector was less than 5 %.

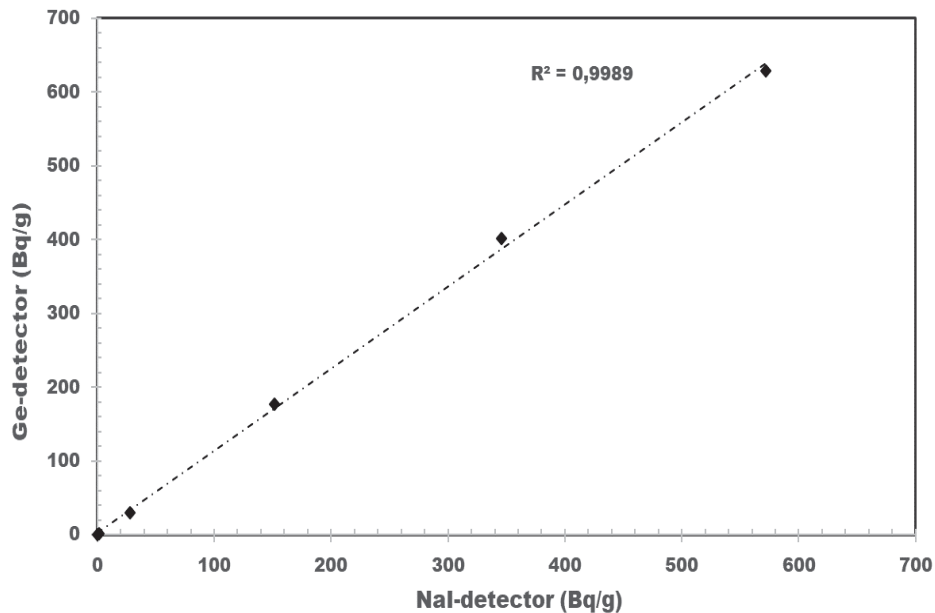


Figure 10: Comparison of <sup>137</sup>Cs measurements between NaI and Ge detectors

### **3.7. Digital autoradiography**

The application of digital autoradiography has proved to be useful in identifying inhomogeneous distributions of radioactivity, and in the task of localizing radioactive particles (Lind, O. et al., 2013; Lind, 2006). Digital autoradiography (also known as digital phosphor imaging or P imaging) is an imaging technique that provides information about the presence and distribution of radioactivity within a sample. Although the type of radionuclide cannot be seen readily, it can provide semi-quantitative information on the presence of radiation, and whether radiation is present as hotspots or more even distribution in a sample. With this technique, a sample is exposed to a reusable phosphor imaging plate (made of photosensitive material), where radiation from the exposed sample reacts with the imaging plate, resulting in the transformation of an image (Reinprecht et al., 2002). Within the imaging plate are photostimulable crystals (made of BaFBr:Eu<sup>2+</sup> in an organic binder), which stores electrons excited by the energy from the radiation. Following exposure, the excited electrons are stored in the crystal lattice, until the plate is scanned with a laser beam that releases the stored energy as luminescence (emission of light), which is finally converted into a digital image. The image produced will show the original pattern of distribution of radiation in the sample. With the aid of an appropriate image analysis software, pixel values of the image can be quantified, since they are proportional to the incident radiation in the sample.

#### *3.7.1. Image acquisition, processing and analysis*

Selected dry samples were screened for heterogeneities using digital autoradiography scanner (HD-CR 35 NDT) together with a digital phosphor imaging plate (Molecular Dynamics, Amersham Pharmacia Biotech). The samples include (1) soil and sediment prior to sequential extraction, (2) residuals from sequential extraction, (3) samples from other sites that were not subjected to sequential extraction, and (4) leaf litter. The litter samples used for autoradiography were air-dried for 24 hours at 60 °C, and the dry weight was determined. Residuals samples were washed with copious amount of water and air-dried. In order to determine the presence of radioactive particles, about 2 g of soil or sediments, 0.5 g litter, and 1 g of residuals were spread thinly in patterns on a double-sided adhesive book binder fixed to pieces of white cardboard over an area of 20 X 10 cm. Each sample had its own designated area marked on the cardboard to aid in localization of the hotspots, in addition to identifying the particular samples from which they originated. Layers of cling film were wrapped around the samples and taped such that sample

integrity was preserved without any problem of cross contamination. The prepared samples were placed under digital phosphor imaging plate inside an exposure cassette. The sealed cassette was kept between lead shields in a dark room to reduce external interferences. Figure 11 provides an overview of the process described above.

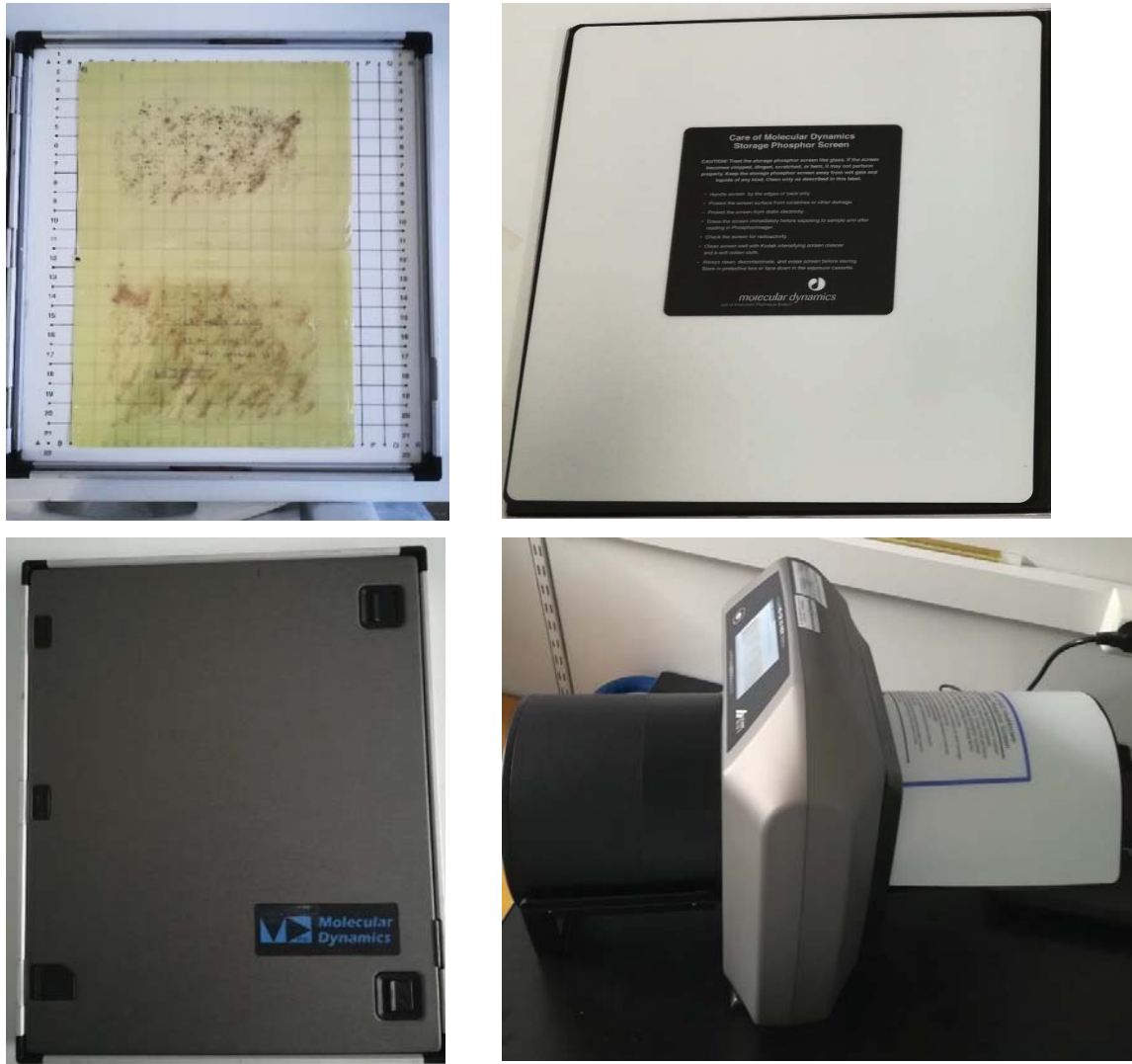


*Figure 11: Overview of processes involved in acquiring image of particles using digital autoradiography. From top (left - prepared sample, right - imaging plate) and bottom (left – exposure cassette, right – digital phosphor plate scanner)*

Exposure times were 3 days for all samples, with the exception of low activity residual samples (triplicates of #10) that were subjected to 1 week of exposure. Images of the distribution and concentration of hotspots (containing radiocesium) in exposed samples were made by scanning the phosphor imaging plate on an image plate scanner (HD-CR 35 NDT). The scanning mode were 50 µm white IP for large plates, and 50 µm Blue IP for small plates to obtain photo-stimulated luminescence (PSL) autoradiography images. The plates were erased after scanning. The presence and distribution of potential radioactive particles were detected in the samples as hotspots after scanning. It must be emphasised that the imaging plates were wiped clean with an intensifying screen cleaner and a soft cotton cloth, followed by erasure on the scanner prior to exposure and after scanning episodes.

Analysis (identification and quantification) of particles was conducted using Fiji (ImageJ) software (Schindelin et al., 2012). Brightness and contrast were adjusted to obtain a clear image for each autoradiogram. Then, the image was inverted and the background signal removed by consistently setting an intensity threshold manually. This is because, in the Image J analysis, it was not feasible to apply the same process to all images, since unequal lighting influenced the extraction by thresholding. Thus, thresholding with one fixed value was not possible in the initial stage of the analysis involving the background, as described in the software manual (Abramoff et al., 2004). A later threshold was set for what would be considered a particle after the background was removed (with a strict limit of 25-5000 pixel area; 0.1-1 sphericity), avoiding samples on the edges of the imaging plate. Intensity surface plots were produced during quantification to show the PSL intensity, which represents the energy deposited per area in association with radiocesium particles. This latter thresholding accounted for high reproducibility, low user bias and low variability.

### **3.8. Statistical analysis**

Statistical analysis of data was performed using MinTab 17 (Minitab Inc.). The Pearson correlation was applied. The criterion for significance was  $p < 0.05$ .

## 4. RESULTS AND DISCUSSION

### 4.1. Soil and sediment characteristics

Table 6 shows values of pH, organic carbon (%), water content (%), total  $^{137}\text{Cs}$  activity concentrations (Bq/g) and percentage of sand, silt, and clay in the seven samples selected from six sampling sites in the near zone (within 11 km radius) of the damaged FDNPP. The pH values ranged from very acidic (4.3) to neutral (7.4), as classified by the French pedological reference base (INRA, 1995; Pansu & Gautheyrou, 2007), with soils and sediments having values of 4.3–7.4 and 4.8–4.9 respectively. Values of the organic matter content were relatively low for all the sites ( $< 20\%$ ), while the water content varied among the sites. With respect to soil and sediment texture, the sand fraction predominates all the sites with values exceeding 60%. The mean values of pH and grain size distribution are indicative of temperate areas with substantial rainfall as it is in Japan with 1000-1600 mm annual precipitation (Konoplev et al., 2016).

The total  $^{137}\text{Cs}$  activity concentration in soils and sediments ranged from 5 to 679 Bq/g, and from 139 to 232 Bq/g respectively. The highest total activity concentration of  $^{137}\text{Cs}$  was observed at station #13, while the lowest was measured at station #10. The wide concentration range of  $^{137}\text{Cs}$  in both soils and sediments reflect the direction of sampling  $^{137}\text{Cs}$ , with samples been collected from both near and far away from the source as well as both inside and outside the main fallout deposition area. This could also be explained by  $^{137}\text{Cs}$  originating from different reactor sources in the course of the nuclear accident. Besides, the fact that the greatest concentration of  $^{137}\text{Cs}$  (679 Bq/g) was observed in soil outside a house 1.3 km between south and southwest of the damaged reactors, and other hotspot samples collected from places where activity were accumulating, indicates that  $^{137}\text{Cs}$  originated from the damaged FDNPP and not from other potential sources like nuclear weapon testing. Other areas where hotspots were observed might have been transported there by water (runoff) which later soaked in the soil or evaporated. Within the FEZ  $^{137}\text{Cs}$  contamination appears to decrease with the distance from the main accident location. Moreover, the values of  $^{137}\text{Cs}$  activity concentrations are comparable to those observed recently by other researchers (Wakiyama et al., 2017).

#### 4.2. Distribution of $^{137}\text{Cs}$ in different grain sizes

The distribution pattern of  $^{137}\text{Cs}$  in the different grain sizes is shown in Figure 12. It appears the content of  $^{137}\text{Cs}$  in each grain size fraction for the samples have decreasing trend with decreasing grain size; from the largest (sand) fractions to the finest (clay) fractions, although the medium-sized (silt) fraction also have a relatively high  $^{137}\text{Cs}$  content. Ideally, a high  $^{137}\text{Cs}$  concentration should have been observed in soil and sediment samples with relatively high clay content, since it is well known that fine particles (such as clays) can contain high amounts of  $^{137}\text{Cs}$  due to their larger surface area for the adsorption of  $^{137}\text{Cs}$  onto the mineral grains. However, this was not so. The existence of majority of  $^{137}\text{Cs}$  in predominantly sand fraction in both soils (50 - 57%) and sediments (61 - 81%) may suggest its strong relation with inert particles, other than clay minerals.

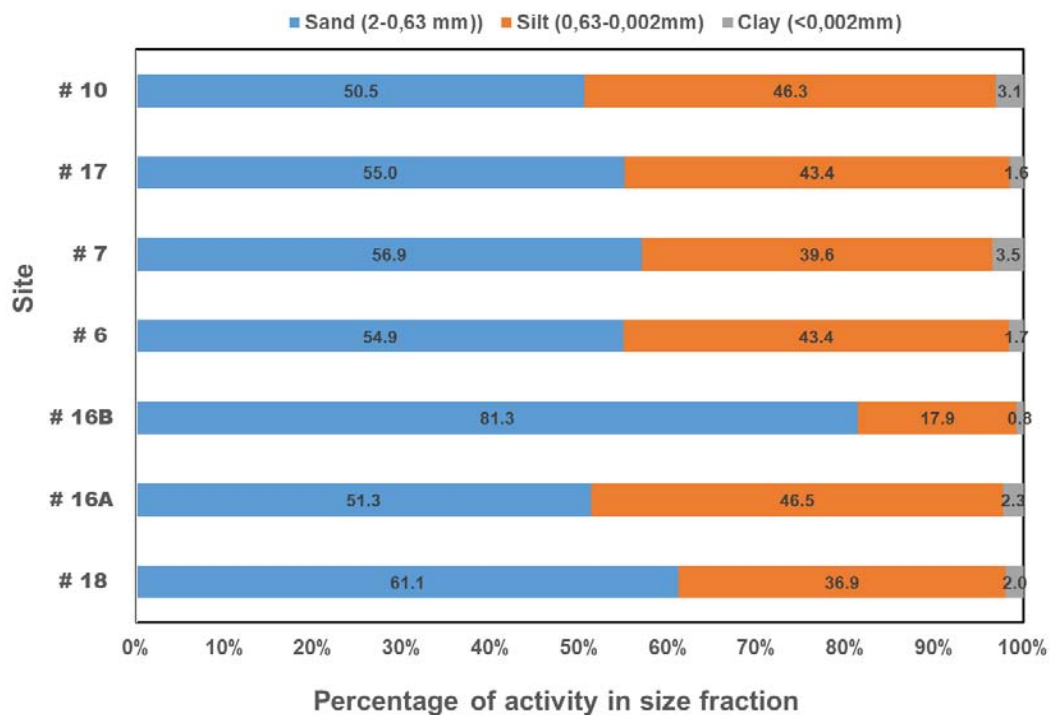


Figure 12: The content of  $^{137}\text{Cs}$  in different grain sizes in the selected sites. Site 6, 7, 10, 16A and 17 are soils while 16B and 18 are sediment

Table 6: Details of soil and sediment samples subjected to sequential extraction procedure

Site #	Location	Sample description	pH	Organic matter (%)	Sand (%)	Silt (%)	Clay (%)	Water content (%)	Activity (Bq/g)
7	1.5 km south/southeast of reactor, concrete platform next to fish factory by the sea	Soil/gravel/sand, 0-5 cm	7.4	5.0	85.7	13.5	0.8	35	390 ± 21
8	1.4 km west/northwest of reactor, concrete ditch outside a house	Black, fine soil from run-off	6.6	15.3	83.7	12.2	4.1	44.2	186 ± 8
10	7.8 km west/southwest of reactor, road into forest, near graveyard	Soil in grass field, 0-6 cm	4.8	6.4	94.7	5.3	0.03	20.9	5 ± 1
13	1.3 km south/southwest of reactor, outside a house	Soil	6.0	10.9	82.6	13.2	4.1	-	680 ± 2
16A	1.4 km west/northwest of reactor, pond between forest and FDNPP	Soil, 0-5 cm	4.3	8.1	92.2	7.8	0.04	26.1	54 ± 3
16B		Surface sediment	4.8	7.7	87.5	12.5	0.02	36.8	139 ± 50
18	4.6 km west/southwest of reactor, fish pond	Surface sediment	4.9	9.6	64.6	34.2	1.2	37.0	232 ± 45

#### **4.3. Distribution of $^{137}\text{Cs}$ in different layers of soils and sediments**

Results of the analysis of the distribution of  $^{137}\text{Cs}$  in different layers of soils and sediments as determined in the initial stage of the bigger project of which this current study is a part are given in Figure 13. This provides an overview on the vertical migration of  $^{137}\text{Cs}$  in soils and sediments. The obtained results profiles show that the  $^{137}\text{Cs}$  has migrated a minimum of 1 cm and a maximum of 10 cm, and all the profiles show a decreasing trend from the top to the layer below. It is well known that 70–90 % of the radiocesium was retained in the fixed form in upper 5–20 cm soil layer regardless of the type of soil and nature of contamination (Gupta & Walther, 2017). Several authors have shown that a major proportion  $^{137}\text{Cs}$  tend to resid within the upper 10 - 15 cm of soils, and that the concentration decrease exponentially with depth (Bunzl et al., 1995; Bunzl et al., 1998; Lee et al., 1997; Schuller et al., 1997). From the results obtained in this study, the sand fraction seems to be abundant with  $^{137}\text{Cs}$  and this appears to vary with depth.

On the basis of concentrations of  $^{137}\text{Cs}$  in topsoil and surface sediment, most of  $^{137}\text{Cs}$  is located in the 0-1 cm. A high activity of  $^{137}\text{Cs}$  in the 0-1 cm layer can be connected with where it was received as a result of the accident. The fact that  $^{137}\text{Cs}$  was also located in the 5-10 cm might be due to percolation of the particles during the postaccident period (in 2011) in response to the high annual rainfall, in addition to soils and sediments having the greatest amount of sand in relation to the other grain sizes. This observation is comparable to research conducted by Kaneko et al. (2015), whereby they found out that aggregation of particles prevented the migration in the vertical direction, since >98% of  $^{137}\text{Cs}$  was retained within the top ~5 cm of the soil, and considered this phenomenon as a key factor controlling the current  $^{137}\text{Cs}$  migration in Fukushima.

According to a report by the National Council on Radiation Protection and Measurements (NCRP), some physical processes such as physical percolation of particles, soil erosion by wind or water, and weathering of particle bound material can move contaminated particles that are not specifically affected by the chemical nature of the matrix into the soil profile (NCRP, 2006). Moreover, sands are known to be relatively pervious to the flow of water due to their large particle size, while the chemical nature of many sands being  $\text{SiO}_2$  make sand nonreactive and insoluble (Kathren, 1984). So,  $^{137}\text{Cs}$  associated to inert particles are likely to travel through sandy soil until they meet barriers or when they become aggregated. This might explain for the

situation encountered whereby the soils and sediment were dominated by sand. So, the vertical movement in the FEZ might have been accelerated by the high amount of rainfall in the Fukushima area, however, the aggregation of particles might have slowed down the migration of particle-associated  $^{137}\text{Cs}$  and not the mechanism of sorbing onto clays. This means that  $^{137}\text{Cs}$  retention will be stronger at shorter depths down the soil/sediment profile, such that  $^{137}\text{Cs}$  cannot reach deeper depths in the short term.

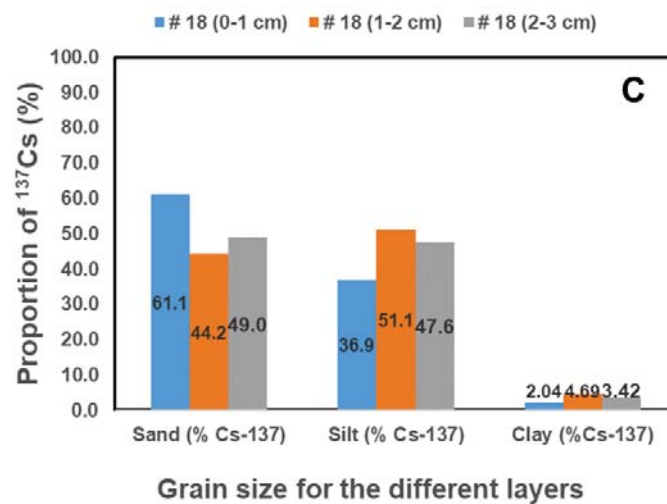
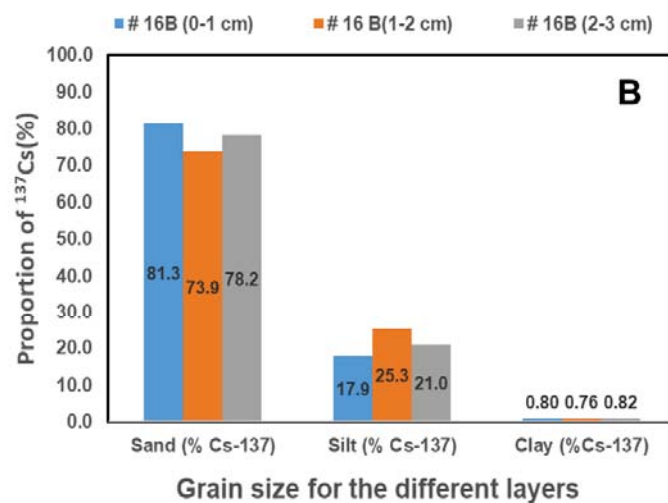
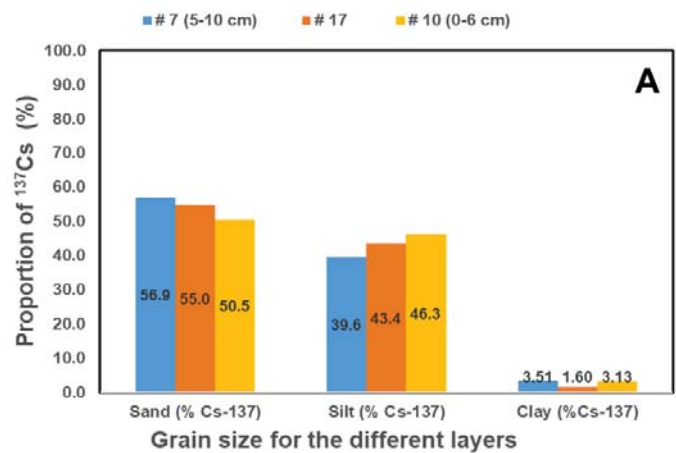


Figure 13. Proportion of  $^{137}\text{Cs}$  contained in the different grain sizes at different levels of soils (A) and sediments (Band C)

#### **4.4. Leaching behaviour of 0.16 M HCl**

Results from the leaching experiment show that majority of  $^{137}\text{Cs}$  (> 96%) could not be extracted with 0.16 M HCl for approximately 65 hours (Figure 14) . Even in the relative proportions of sand, silt and clay,  $^{137}\text{Cs}$  could still not be extracted, except for an anomaly encountered in #16A for clay fraction. The highest  $^{137}\text{Cs}$  extraction from the 10 samples was <3% . The fact that a greater proportion of  $^{137}\text{Cs}$  was not leached by 0.16 M HCl in approximately 65 hours suggests that  $^{137}\text{Cs}$  is either strongly bound to the soil/sediment particles or that  $^{137}\text{Cs}$  is present in the form of inert particles. The latter explanation is more plausible upon comparing the result over here with what was obtained during sequential extraction, as they are in good agreement. So, particle-associated  $^{137}\text{Cs}$  can be said to exhibit low potential mobility and bioavailability in the FEZ. Perhaps, information on the long term potential mobility of particle associated  $^{137}\text{Cs}$  could be possible if the extraction had continued for one week (168 hours) as pointed out by some authors (Lind et al., 2009).

It should be recognized that potential adverse consequences of particle associated  $^{137}\text{Cs}$  rest on the premise of bioavailability from the contaminated soil and sediments in the FEZ. Although the area could present potential risk to humans and animals via external radiation, it would be assumed not to be much of a concern considering the fraction of  $^{137}\text{Cs}$  that could be accessed via internal organs. It is likely that when contaminated soil or radioactive particle is ingested, the  $^{137}\text{Cs}$  will not be completely absorbed into the body, since a greater percentage of  $^{137}\text{Cs}$  is not dissolved by 0.16 M HCl. Moreover, given the relatively short biological half-life of  $^{137}\text{Cs}$  in animals and humans, the potential particle-associated  $^{137}\text{Cs}$  is expected to be excreted when ingested. Thus, the fraction not dissolved and absorbed (which in this case forms a greater proportion) will eventually be expelled from the digestive system along with other solid or liquid waste. Nevertheless, some researchers have shown that radioactive particles were retained in the gut of ruminants (Beresford et al., 1992; Beresford et al., 2000) during passage, delivering doses to nearby internal organs. So, potential radiological implications may arise due to failure or inefficiency of the affected animal or person to excrete the particle upon lodging in the GI tract.

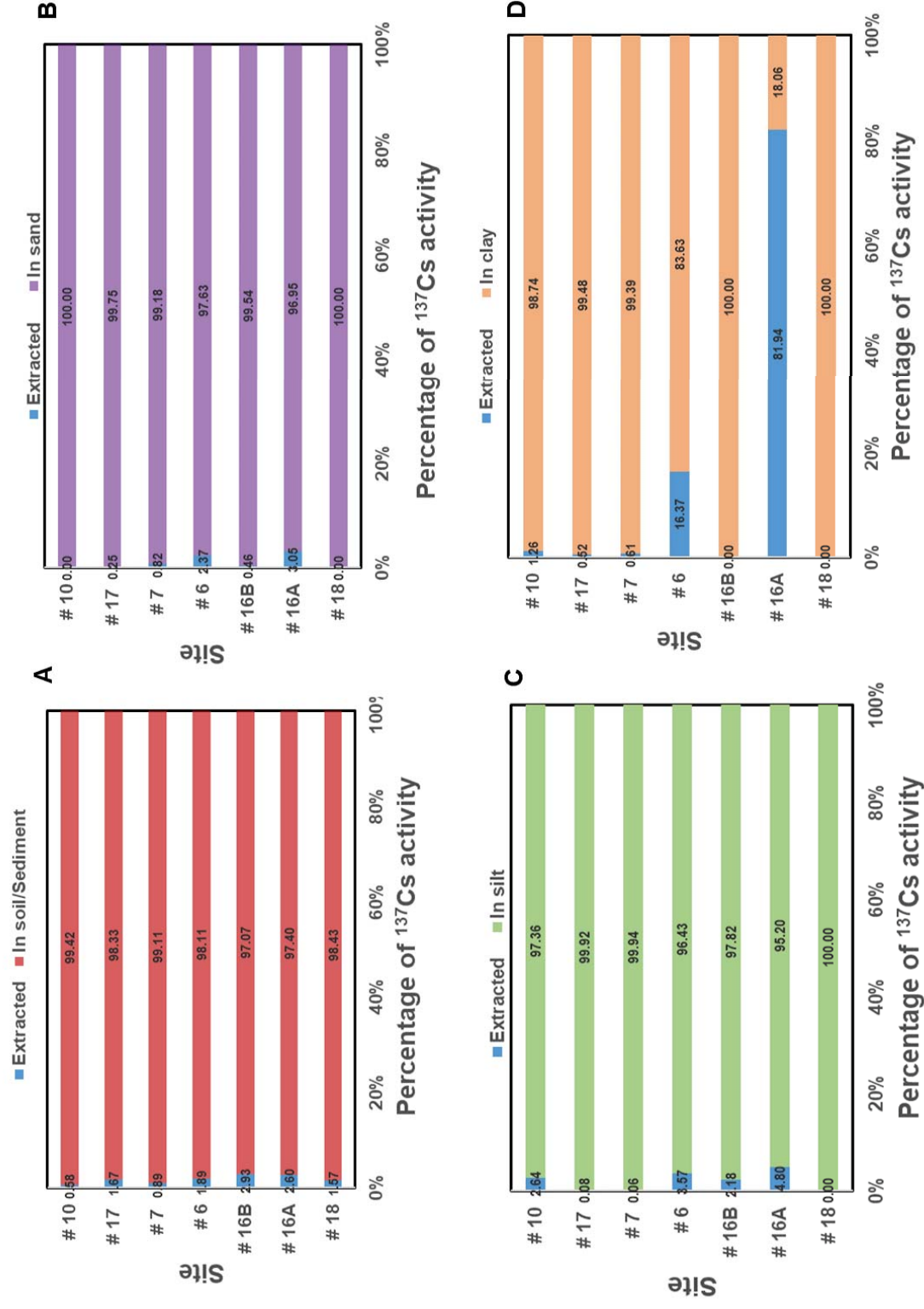


Figure 14: Proportion of  $^{137}\text{Cs}$  leached in (A) total samples before size-segregation, (B) sand fraction, (C) silt fraction, and (D) clay fraction. Site 6, 7, 10, 16A and 17 are soils while 16B and 18 are sediments

#### 4.5. Sequential extraction of $^{137}\text{Cs}$ from soils and sediments

The analytical results of  $^{137}\text{Cs}$  fractionation in five soils and two sediments obtained from six sites is summarised graphically in Figure 15, while the detailed data is presented in Table 1A in the Appendix.

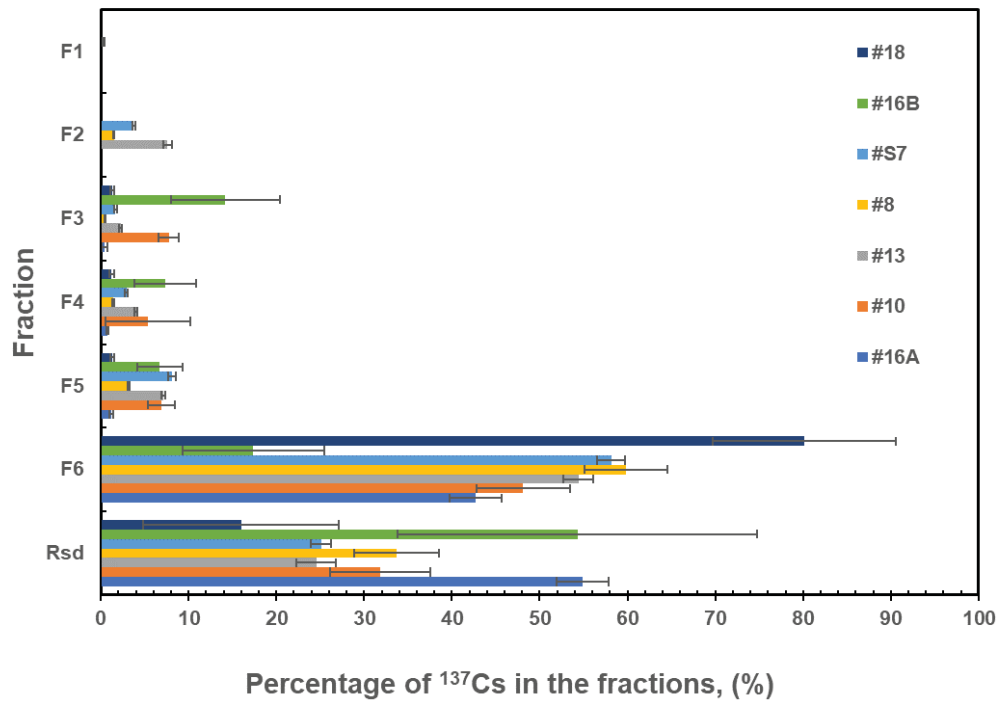


Figure 15: : Percentage distribution of  $^{137}\text{Cs}$  in the fractions from sequential extraction of five soils and two fresh sediments from the 11 km zone in FDNPP area.

In Figure 15, the abscissa corresponds to  $^{137}\text{Cs}$  in the fractions (%) against its total inventory in a given soil or sediment sample for each extraction step or the residue (Rsd). For both soil and sediment samples,  $^{137}\text{Cs}$  was mainly contained in the extract of the strong acid dissolution (7 M  $\text{HNO}_3$ ) that is fraction F6, with the exception of samples from site #16. Generally, the fractions of  $^{137}\text{Cs}$  in the ion exchange extract (F2), those originating from amorphous carbonates (F3) and reductive dissolution (F4), in addition to those corresponding to organic dissolution (F5) were all below 20% for both soils and sediments. Interestingly, a relatively high fraction of  $^{137}\text{Cs}$  (16–55 %) remained in the residual fraction (Rsd) after treating with 7 M  $\text{HNO}_3$  at 80 °C. Meanwhile, there was virtually no  $^{137}\text{Cs}$  extracted in the water soluble fraction (F1), and this could be attributed to the high amount of rainfall in the FDNPP area that might have resulted in this

fraction been carried in surface runoff to other areas. The results presented in Figure 15 is in qualitative agreement with those observed by other researchers (Saito et al., 2014), significant proportion of  $^{137}\text{Cs}$  was in the strong acid dissolution fraction. Sequential extraction results obtained by Kanai (2011) prior to the FDNPP accident indicated that  $^{137}\text{Cs}$  was mainly contained in silicate fraction, which is contrary to results obtained after the accident. This gives an indication of  $^{137}\text{Cs}$  mainly in inert form after after the accident.

In assessing the strength of binding as well as the mobility and bioavailability of  $^{137}\text{Cs}$  in the FEZ, the sum of  $^{137}\text{Cs}$  extracted in the first three steps, i.e., those constituting water soluble, exchangeable and carbonates bound fractions ( $F1+F2+F3$ ) was considered mobile and hence potentially bioavailable. Subsequently, the sum of extracts from reductive, organic and strong acid dissolution ( $F4+F5+F6$ ) constitute immobile fraction, which can be considered as potentially not bioavailable. The remaining residual fraction ( $R_{sd}$ ) were categorised as inert fraction. Analysis of the results showed that  $^{137}\text{Cs}$  is generally irreversibly bound in soils (45–69 %) and sediments (32–83 %) as presented in Figure 16. This suggest relatively low mobility and potential bioavailability under natural conditions in FEZ. Moreover, given that the strong acids used for the experiments could not dissolve the  $^{137}\text{Cs}$  particles, this means that  $^{137}\text{Cs}$  has a lower propensity to change into more available forms in the short term.

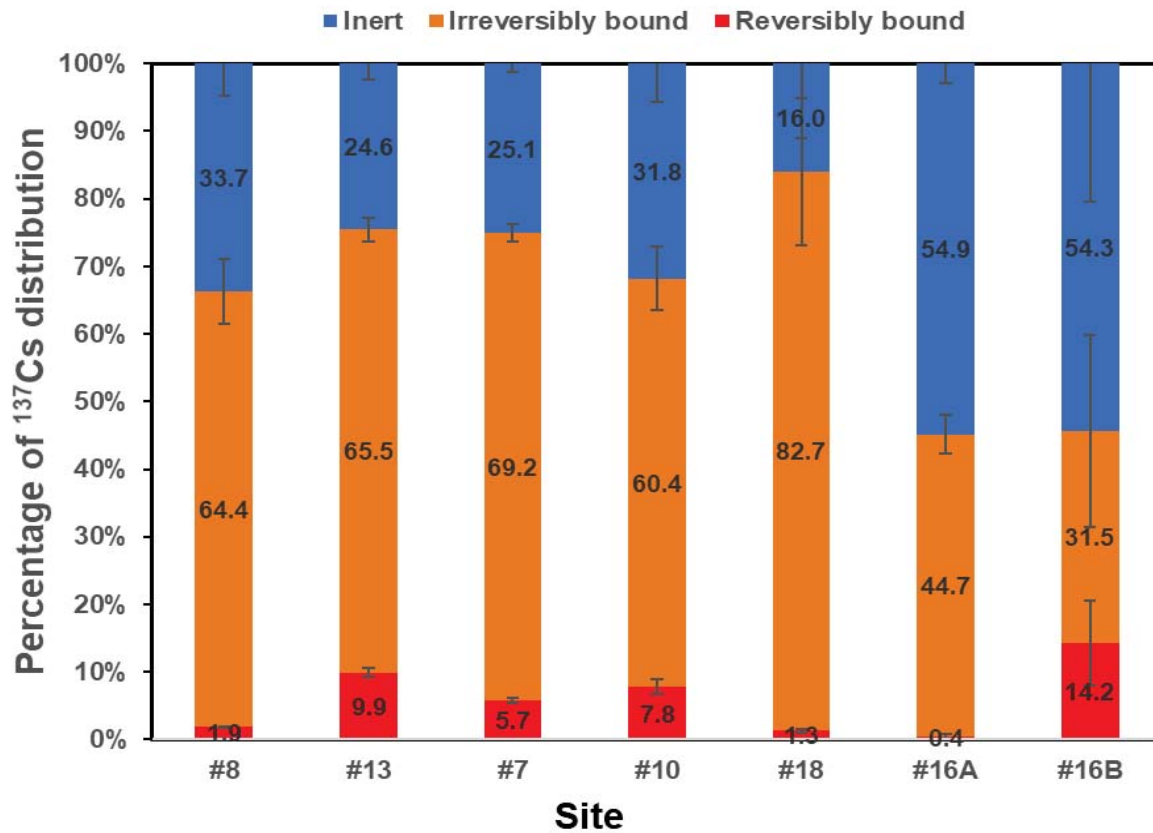


Figure 16: Fractionation of  $^{137}\text{Cs}$  in soils and sediments as a fraction of the total activity following sequential extraction. Site 7, 8, 10, 13 and 16A are soils while 16B and 18 are sediments

Although  $^{137}\text{Cs}$  can generally be considered immobile and potentially not bioavailable in FEZ, the relative proportions of  $^{137}\text{Cs}$  in the reversibly bound fractions in soils (0.4–10 %) and pond sediments (1.3 – 14 %) associated with mobile and bioavailable fractions cannot be ignored due to the rather high total activity concentrations measured at these sites, especially #13 (see Table 1A in the appendix). Moreover, since the potential environmental risk of  $^{137}\text{Cs}$  in soils and sediments is associated with both the total activity content (especially for external radiation) and speciation of  $^{137}\text{Cs}$ , these relatively low reversibly bound values could be of importance. It is possible that these relatively small fraction of mobile and bioavailable  $^{137}\text{Cs}$  present in soil and sediments could pose certain health risks. This could be particularly important especially for cryptophytes and hemicryptophytes plants, whose renewal gemmae are located on the soil surface or buried into the topsoil (Pozolotina et al., 2012), in addition to megafauna such as earthworms and small vertebrates.

#### 4.6. Estimating radioactive particles from total samples and residual fractions

Digital autoradiography has been successfully used to screen environmental samples for heterogeneities of anthropogenically derived radioactivity (Itoh et al., 2014; Lind, 2006; Lind et al., 2009; Lind, O. C. et al., 2013). In this present work, the use of digital autoradiography clearly demonstrates heterogeneous distributions of radioactivity in all investigated samples based on the observation of hotspots that were significantly different from the matrix background. Digital autoradiography of soils and sediments before and after sequential extraction showed signals that appeared to be radioactive particles, giving indications of heterogeneities in all samples, as represented in Figure 17.

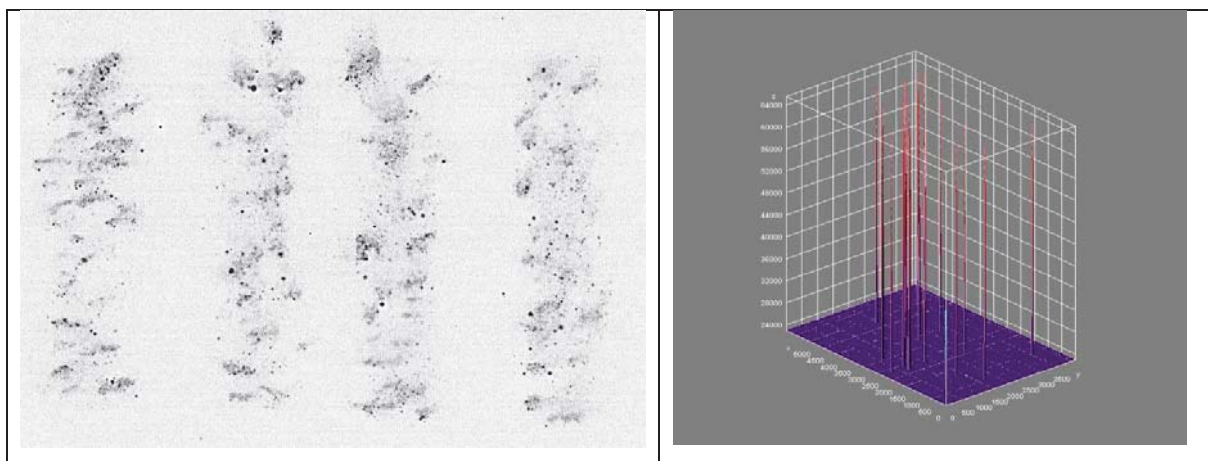


Figure 17: Representative autoradiogram showing hotspots, along with its surface plots

From this work, all the autoradiograms show a high number of hotspots believed to be potential radioactive particles. The radioactive particles located by the autoradiography was confirmed with  $\gamma$ -ray spectrometer to ensure that they contain  $^{137}\text{Cs}$ , since natural radionuclides like  $^{40}\text{K}$ , uranium, or the thorium series can also excite imaging plates (Mukai et al., 2014). Although the presence of heterogeneities were confirmed, individual radioactive particles were not isolated for further characterization at the time of preparing this report. Isolation and detailed characterization of the particles using solid state speciation techniques is a subject for future work.

Analysis of the autoradiograms show a relatively high number of particle per gram of sample (Table 7). Notwithstanding, the samples that showed high variability were those having what seems to be like aggregates of soil/sediment. The method used over here determines area occupied by the particles, but not differentiating the particles. This will require further analysis using solid state speciation techniques, which is part of the broader project, but outside the scope of this report. In addition, analysis of hot particle associated with the fallout, and Cs isotope ratios reflecting different burnup could help explain the origin of these particles in relation to the damaged FDNPP reactors. Notwithstanding, the potential particle found strengthened the hypothesis of particle-associated radiocesium as the source of the unexpected speciation of  $^{137}\text{Cs}$ .

Several reports highlight the need for adequately accounting for radioactive particles in soil and sediments. As at August 2018, a search through literature revealed that only two papers attempted to quantify radioactive particles.

are different from those that have been previously studied...

provide basis for estimating quantitatively

Table 7: The number of radioactive particles per gram of dry mass of sample before (total) and after (residue) sequential extraction (S.E)

Site (#)	Sample description	Particles/g	
		Total (before S.E)	Residue (After S.E)
1	soil, 0-3 cm	52 ± 3	
1	litter	42 ± 15	
4	litter	28 ± 3	
4	soil, 0-6 cm	41 ± 16	
5	soil, 0-6 cm	33 ± 8	
6	soil, 0-3 cm	46 ± 6	
7	soil/gravel/sand, 5-10 cm	59 ± 4	
7	soil/gravel/sand, 0-5 cm	68 ± 10	9 ± 2
8	black, fine soil from run-off	81 ± 7	6 ± 0
9	soil/gravel, 0-2.5 cm	19 ± 8	
10	soil, 0-6 cm	70 ± 7	2 ± 1
13	soil	77 ± 4	11 ± 4
14	soil, top layer	128 ± 34	
16A	soil, 0-5 cm	53 ± 3	7 ± 1
16B	surface sediment	32 ± 1	12 ± 3
17	soil, 0-20 cm	136 ± 0	
18	surface sediment	69 ± 1	9 ± 6

A higher number of particles were counted from autoradiogram analysis prior to sequential extractions, however, the number of radioactive particles reduced considerably for the samples subjected to sequential extractions. Reduction in the number of radioactive particles may suggest that some of the particles were dissolved by the sequential extraction process. Alternatively, it could mean that those counted initially as radioactive particles prior to sequential extraction were aggregates of soil particles bearing radiocesium and not necessarily “hot particles”. The method of quantification used over here is the first of its kind. A recent (August 2018) search through the abundant literature emphasizing the need to account for cesium radioactive particles in soil and

sediments, on two attempted (Ikehara et al., 2018; Itoh et al., 2014) to quantify radioactive particles using their unique methods. While Ikehara et al. (2018) distinguished between cesium microparticles and cesium particles sorbed on the frayed edge site of clays, the method is to some extent hypothetical, while the method used in this study is based on real experiment. Unique to the method in this study is the quantification of cesium bearing radioactive particles before and after sequential extractions. By setting a threshold what appear to be aggregation of radiocesium sorbing to clays were removed for real particles to be counted. While the limit of detection was not determined, calibration in the future work could make this possible. The results obtained in this study using our unique method is similar to results obtained using the method developed by Ikehara et al. (2018). Calibration of our method will result in a producing a novel method for quantification of cesium microparticles.

Confirmation by further isolation and characterization will be carried out in the future work. Notwithstanding, the number of radioactive particles differ among the various samples analysed in this study, and it appears to be closely related to direction of the plume (Fig. 18), and perhaps, the different source reactors. The latter explanation may require obtaining atom ratios by mass spectrometry (e.g. ICP-QQQ (triple quad) MS) and use it for release source identification.

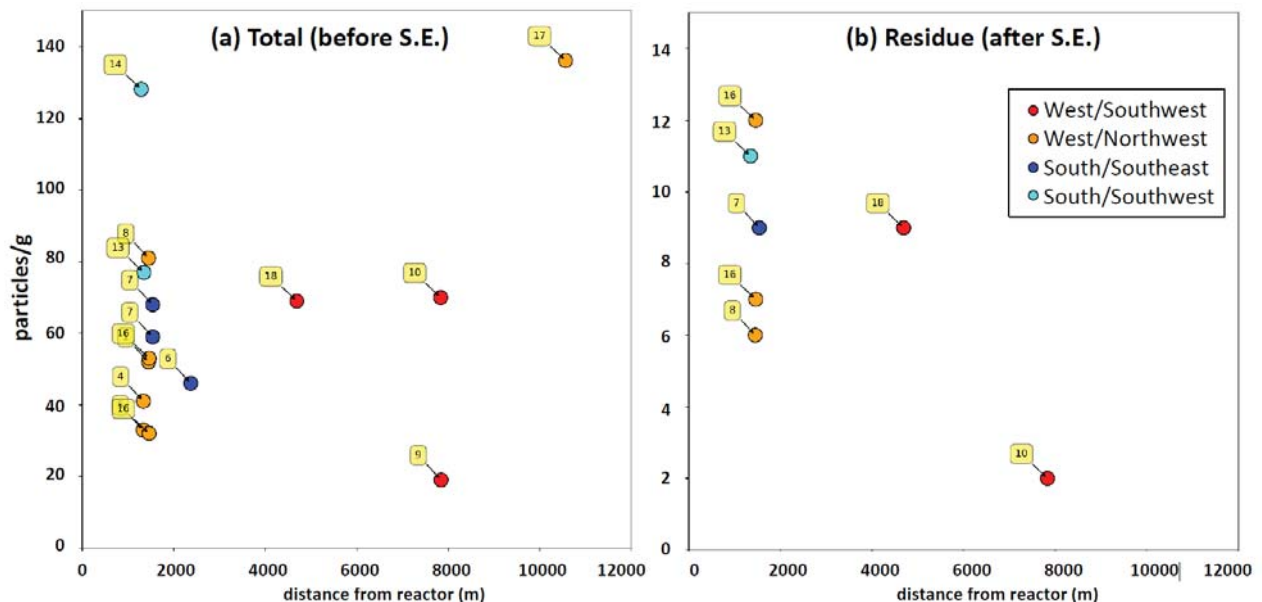


Figure 18: Number of particles per gram of dry mass as a function of distance and direction to the reactor in (a) total and (b) residue form sequential extraction. The numbers are for the various sites, while the colour represent direction.

The studied sites have shown that  $^{137}\text{Cs}$  containing particles decreases with increasing distance from the epicenter of the accident. Therefore the soil and sediments in areas close to the damaged FDNPP are contaminated with  $^{137}\text{Cs}$  to a greater extent than those of the adjacent areas a little further away. This is reflection of the deposition patterns of fallout  $^{137}\text{Cs}$ .

Since this work is part of a larger project, it may be followed with detailed characterization. Scanning electron microscopy (SEM) interfaced with surface sensitive X-ray microanalysis (XRMA) will be used to provide information on radiocesium distribution and characterization of radioactive particle surface structures (Salbu et al., 2001b). By using backscattered electron imaging mode (BEI), particle surfaces containing high atomic number elements will appear as bright localized areas, while X-ray mapping will give information on the 2D elemental distribution on individual particle surfaces. Also, the sensitivity for X-ray fluorescence mapping can be increased using a polychromatic synchrotron beam. A number of synchrotron based X-ray microscopic techniques available for characterizing radioactive particles using microbeams (Salbu, 2009b). Information on 2D or 3D elemental distribution within individual particles will be obtained from microscopic X-ray fluorescence analysis ( $\mu$ -XRF) analysis, while micro-X-ray diffraction ( $\mu$ -XRD) will provide information on crystallographic structures of solid particles. Furthermore, extended X-ray absorption fine structure (EXAFS) analysis will provide information on the coordination number and the distance to neighbouring atoms within the solid. Finally, volume distribution of radiocesium within particles and information on porosity be obtained with  $\mu$ -tomography.

#### **4.7. Assessing the influence of soil/sediment characteristics on binding mechanism of $^{137}\text{Cs}$**

Some authors have linked soil clay content with cesium bioavailability, through a sequence of controls (Smith & Comans, 1996; Smith et al., 2000; Smith et al., 1999). This is reflected in the notion that the mobility and bioavailability  $^{137}\text{Cs}$  over the first few years after fallout is controlled by the fixation of  $^{137}\text{Cs}$  into clay mineral lattice (e.g. illite). So, this fixation process is explained to exert control over the amount of radiocesium in soil water and therefore its

availability to terrestrial biota and for transfer to rivers and lakes. However, the particle issue is largely ignored.

In assessing the influence of soil/sediment characteristics on the binding mechanism of  $^{137}\text{Cs}$  in FEZ, there was no correlation ( $R^2 = 0.15 - 0.36$ ) between silt and clay content in the soils and sediments and the activity concentration of  $^{137}\text{Cs}$  for irreversible and inert fractions. This is in sharp contrast to the explanation offered by Kaneko et al. (2015) regarding the inert fractions. According to Kaneko et al. (2015), the inertness of  $^{137}\text{Cs}$  in Fukushima soils is due to adsorption onto submicron-sized sheet aluminosilicates. However, in this study, fixation of  $^{137}\text{Cs}$  into clays appears not to be the main reason for the high immobile fraction, as there are inert particles. On the basis of this general observation, coupled with the apparent lack of clays, in addition to the lack of correlation between the soils and sediments and the activity concentration of  $^{137}\text{Cs}$  for irreversible and inert fractions, may indicate that  $^{137}\text{Cs}$  is mainly in the form of inert particles as evidenced by relatively high inert fractions. From the observed result on mobility of  $^{137}\text{Cs}$ , it clearly shows that  $^{137}\text{Cs}$  is associated with inert particles.

#### **4.8. Influence of radioactive particle on $^{137}\text{Cs}$ speciation**

A direct link between radioactive particles and speciation of  $^{137}\text{Cs}$  was established (Figure 19) as evidenced by a strong positive Pearson correlation ( $r = 0.76$ ) between activity concentration of inert particles and the number of particles per gram of samples after sequential extractions (residue). Moreover, a very strong evidence ( $p \leq 0.001$ ) was observed that the number of particles per sample were significantly different, thereby lending credence to the hypothesis of heterogenous distribution of radioactive particles.

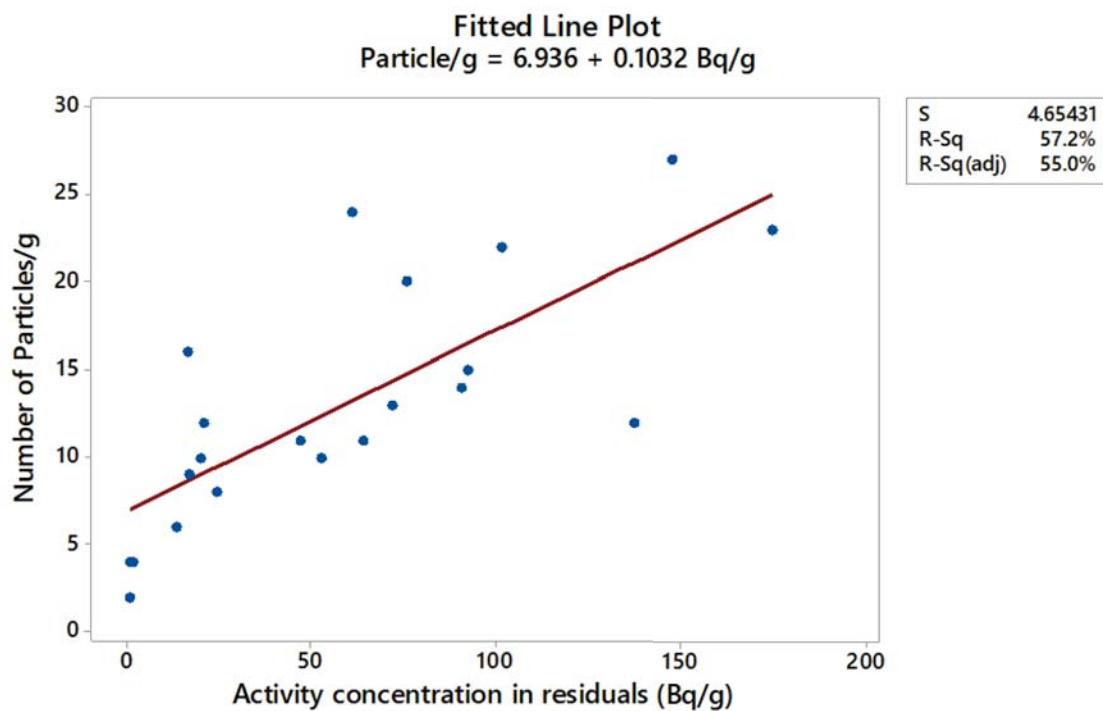


Figure 19: Correlation between Activity concentration in residuals and number of particles from residuals after sequential extraction

From the analysis, it seems radioactive particles potentially exert a significant influence on the speciation in the 11 km FEZ that is otherwise considered to be dominated by mineralogical characteristics (specifically, clay). This suggest that the weathering of particles will control mobility and migration of particle-associated  $^{137}\text{Cs}$  in the FEZ.

## 5. CONCLUSION

The FDNPP accident in March 2011 at the nuclear facilities of units 1, 2 and 3 in Japan led to the contamination of the FEZ and beyond with radioactive cesium containing particles. The complex nature of soil and sediment contamination was studied. Very heterogeneous distributions of  $^{137}\text{Cs}$  was encountered indicating the presence of radioactive particles. It was clear that the soils and sediments of the studied sites in the FEZ have a concentration of significant amount of  $^{137}\text{Cs}$  mainly located in the immobile phase. The content of  $^{137}\text{Cs}$  in the layers of soil and sediments revealed a general decreasing trend. It is caused mainly by reduction of  $^{137}\text{Cs}$  mobility in the soil due to a larger proportion of inert forms. The distribution of  $^{137}\text{Cs}$  in the soil and sediment demonstrated that  $^{137}\text{Cs}$  migration may depend on particle size, grain size and environmental factors like rainfall and landscape.

Results of  $^{137}\text{Cs}$  speciation in soil and sediment investigated by sequential extraction showed that most of  $^{137}\text{Cs}$  in soil and sediment remains largely irreversibly bound and is associated to inert fraction. The fraction of soluble  $^{137}\text{Cs}$  in the contaminated soil and sediment comprises a minor part and varies with the distance from the reactor, but appears to be in the direction of the plume. From this study it can be concluded that  $^{137}\text{Cs}$  is generally less mobile and potentially less bioavailable in FEZ. Furthermore, radioactive particles exerted certain influence on  $^{137}\text{Cs}$  mobility and bioavailability. Meanwhile, the study of  $^{137}\text{Cs}$  in the contaminated soil and sediments suggest that adsorption processes may not have been the main controlling mechanism. From the observed mobility of  $^{137}\text{Cs}$ , it clearly shows that the behaviour of  $^{137}\text{Cs}$  in FEZ is controlled by inert particles.

To predict the future dynamics of particle bearing  $^{137}\text{Cs}$ , continuous study of  $^{137}\text{Cs}$  would be beneficial. The isotopic ratio of  $^{137}\text{Cs}$  and  $^{133}\text{Cs}$  in the extract by strong-acid dissolution, and those in the extracts by water, ion exchange, and reductive dissolution could help explain if a steady state has been reached or not. Moreover, information on the solid state speciation of  $^{137}\text{Cs}$  will improve the basis for assessing environmental impact of Fukushima derived particles. Finally, to more readily reveal the fraction of the total Cs derived from the Fukushima source reactors, it will be important to know the initial Cs-135/Cs-137 activity ratio.

## References

- Abe, Y., Iizawa, Y., Terada, Y., Adachi, K., Igarashi, Y. & Nakai, I. (2014). Detection of uranium and chemical state analysis of individual radioactive microparticles emitted from the Fukushima nuclear accident using multiple synchrotron radiation X-ray analyses. *Analytical chemistry*, 86 (17): 8521-8525.
- Abràmoff, M. D., Magalhães, P. J. & Ram, S. J. (2004). Image processing with ImageJ. *Biophotonics international*, 11 (7): 36-42.
- Adachi, K., Kajino, M., Zaizen, Y. & Igarashi, Y. (2013). Emission of spherical cesium-bearing particles from an early stage of the Fukushima nuclear accident. *Scientific reports*, 3: 2554.
- Admon, U. (2009). Single Particles Handling and Analyses. In *Radioactive Particles in the Environment*, pp. 15-55. Dordrecht: Springer Netherlands.
- ATSDR. (2004). Toxicological profile for Cesium. *Agency for Toxic Substances and Disease Registry, Atlanta, GA: U.S. Department of Health and Human Services, Public Health Service*.
- Atwood, D. A. (2013). *Radionuclides in the Environment*: John Wiley & Sons.
- Ault, A. P., Peters, T. M., Sawvel, E. J., Casuccio, G. S., Willis, R. D., Norris, G. A. & Grassian, V. H. (2012). Single-particle SEM-EDX analysis of iron-containing coarse particulate matter in an urban environment: sources and distribution of iron within Cleveland, Ohio. *Environmental science & technology*, 46 (8): 4331-4339.
- Avery, S. V. (1996). Fate of caesium in the environment: Distribution between the abiotic and biotic components of aquatic and terrestrial ecosystems. *Journal of Environmental Radioactivity*, 30 (2): 139-171. doi: [https://doi.org/10.1016/0265-931X\(96\)89276-9](https://doi.org/10.1016/0265-931X(96)89276-9).
- Bakken, L. R. & Olsen, R. A. (1990). Accumulation of radiocaesium in fungi. *Canadian journal of microbiology*, 36 (10): 704-710.
- Beresford, N., Lamb, C., Mayes, R., Howard, B. & Colgrove, P. (1989). The effect of treating pastures with bentonite on the transfer of <sup>137</sup>Cs from grazed herbage to sheep. *Journal of Environmental Radioactivity*, 9 (3): 251-264.
- Beresford, N. & Howard, B. (1991). The importance of soil adhered to vegetation as a source of radionuclides ingested by grazing animals. *Science of the Total Environment*, 107: 237-254.
- Beresford, N., Mayes, R., Howard, B., Eayres, H., Lamb, C., Barnett, C. & Segal, M. (1992). The bioavailability of different forms of radiocaesium for transfer across the gut of ruminants. *Radiation Protection Dosimetry*, 41 (2-4): 87-91.
- Beresford, N. A., Mayes, R. W., Cooke, A. I., Barnett, C. L., Howard, B. J., Lamb, C. S. & Naylor, G. P. L. (2000). The importance of source-dependent bioavailability in determining the transfer of ingested radionuclides to ruminant-derived food products. *Environmental science & technology*, 34 (21): 4455-4462.
- Brückmann, A. & Wolters, V. (1994). Microbial immobilization and recycling of <sup>137</sup>Cs in the organic layers of forest ecosystems: relationship to environmental conditions, humification and invertebrate activity. *Science of the total environment*, 157: 249-256.
- Bunzl, K., Kracke, W., Schimmack, W. & Auerswald, K. (1995). Migration of fallout <sup>239+240</sup>Pu, <sup>241</sup>Am and <sup>137</sup>Cs in the various horizons of a forest soil under pine. *Journal of Environmental Radioactivity*, 28 (1): 17-34.
- Bunzl, K., Kracke, W., Schimmack, W. & Zelles, L. (1998). Forms of fallout <sup>137</sup>Cs and <sup>239+240</sup>Pu in successive horizons of a forest soil. *Journal of Environmental Radioactivity*, 39 (1): 55-68.
- Chino, M., Nakayama, H., Nagai, H., Terada, H., Katata, G. & Yamazawa, H. (2011). Preliminary Estimation of Release Amounts of <sup>131</sup>I and <sup>137</sup>Cs Accidentally Discharged from the Fukushima Daiichi Nuclear Power Plant into the Atmosphere. *Journal of Nuclear Science and Technology*, 48 (7): 1129-1134. doi: 10.1080/18811248.2011.9711799.

- Comans, R. N., Middelburg, J. J., Zonderhuis, J., Woittiez, J. R., De Lange, G. J., Das, H. A. & Van Der Weijden, C. H. (1989). Mobilization of radiocaesium in pore water of lake sediments. *Nature*, 339 (6223): 367.
- Comar, C. L. (1955). *Radioisotopes in biology and agriculture*: McGraw-Hill: London.
- Council, N. R. (2003). *Bioavailability of contaminants in soils and sediments: processes, tools, and applications*: National Academies Press.
- Darley, J. P., W. Charles, M., P. Fell, T. & D. Harrison, J. (2003). Doses and risks from the ingestion of Dounreay fuel fragments. *Radiation Protection Dosimetry*, 105 (1-4): 49-54. doi: 10.1093/oxfordjournals.rpd.a006288.
- Dubchak, S. (2017). Distribution of Caesium in Soil and its Uptake by Plants. In *Impact of Cesium on Plants and the Environment*, pp. 1-18: Springer.
- Ehlers, L. J. & Luthy, R. G. (2003). *Peer reviewed: contaminant bioavailability in soil and sediment*: ACS Publications.
- Golder Associates. (2016). Accounting for Bioavailability in Contaminated Land Site-Specific Health Risk Assessment. (Report Number: 1542820-003-R-Rev0).
- Guillén, J., Baeza, A. & Salas, A. (2012). Speciation of Radionuclides in Aquatic and Terrestrial Ecosystems. In Gerada, J. G. (ed.) *Radionuclides: Sources, Properties and Hazards*, pp. 95-112. Hauppauge: Hauppauge : Nova Science Publishers, Inc.
- Gupta, D. K. & Walther, C. (2017). *Impact of Cesium on Plants and the Environment*: Springer.
- Heinrich, G. (1992). Uptake and transfer factors of <sup>137</sup>Cs by mushrooms. *Radiation and environmental biophysics*, 31 (1): 39-49.
- Hirose, K. (2012). 2011 Fukushima Dai-ichi nuclear power plant accident: summary of regional radioactive deposition monitoring results. *Journal of environmental radioactivity*, 111: 13-17.
- Howard, B., Beresford, N. & Hove, K. (1991). Transfer of radiocesium to ruminants in natural and semi-natural ecosystems and appropriate countermeasures. *Health Physics*, 61 (6): 715-725.
- Huang, Y., Kaneko, N., Nakamori, T., Miura, T., Tanaka, Y., Nonaka, M. & Takenaka, C. (2016). Radiocesium immobilization to leaf litter by fungi during first-year decomposition in a deciduous forest in Fukushima. *Journal of environmental radioactivity*, 152: 28-34.
- Huheey, J. E., Keiter, E. A., Keiter, R. L. & Medhi, O. K. (2006). *Inorganic chemistry: principles of structure and reactivity*: Pearson Education India.
- IAEA. (2011a). Radioactive Particles in the Environment: Sources, Particle Characteristics, and Analytical Techniques. *IAEA-TECDOC-1663*, Vienna, 32: 90.
- IAEA. (2011b). *Radioactive Particles in the Environment: Sources, Particle Characterization and Analytical Techniques*. IAEA TECDOC Series, 1663. Vienna: INTERNATIONAL ATOMIC ENERGY AGENCY. p. 90.
- IAEA. (2014). Guidelines for Using Fallout Radionuclides to Assess Erosion and Effectiveness of Soil Conservation Strategies. *IAEA-TECDOC 1741*: 226.
- Ikehara, R., Suetake, M., Komiya, T., Furuki, G., Ochiai, A., Yamasaki, S., Bower, W. R., Law, G. T., Ohnuki, T. & Grambow, B. (2018). Novel Method of Quantifying Radioactive Cesium-Rich Microparticles (CsMPs) in the Environment from the Fukushima Daiichi Nuclear Power Plant. *Environmental science & technology*.
- INRA. (1995). Référentiel pédologique. Association Française d'étude des sols. INRA, 332 p
- Itoh, S., Eguchi, T., Kato, N. & Takahashi, S. (2014). Radioactive particles in soil, plant, and dust samples after the Fukushima nuclear accident. *Soil science and plant nutrition*, 60 (4): 540-550.

- Jaeschke, B. C., Lind, O. C., Bradshaw, C. & Salbu, B. (2015). Retention of radioactive particles and associated effects in the filter-feeding marine mollusc *Mytilus edulis*. *Science of the Total Environment*, 502: 1-7.
- Kanai, Y. (2011). Characterization of <sup>210</sup>Pb and <sup>137</sup>Cs radionuclides in sediment from Lake Shinji, Shimane Prefecture, western Japan. *Applied Radiation and Isotopes*, 69 (2): 455-462. doi: <https://doi.org/10.1016/j.apradiso.2010.09.019>.
- Kaneko, M., Iwata, H., Shiotsu, H., Masaki, S., Kawamoto, Y., Yamasaki, S., Nakamatsu, Y., Imoto, J., Furuki, G. & Ochiai, A. (2015). Radioactive Cs in the severely contaminated soils near the Fukushima Daiichi nuclear power plant. *Frontiers in Energy Research*, 3: 37.
- Kashparov, V., Oughton, D., Zvarich, S., Protsak, V. & Levchuk, S. (1999). Kinetics of fuel particle weathering and <sup>90</sup>Sr mobility in the Chernobyl 30-km exclusion zone. *Health Physics*, 76 (3): 251-259.
- Kashparov, V., Lundin, S., Zvarych, S., Yoshchenko, V., Levchuk, S., Khomutinin, Y. V., Maloshtan, I. & Protsak, V. (2003). Territory contamination with the radionuclides representing the fuel component of Chernobyl fallout. *Science of the Total Environment*, 317 (1-3): 105-119.
- Kathren, R. L. (1984). *Radioactivity in the environment: sources, distribution, and surveillance*: Harwood Academic Publishers.
- Kennedy, V., Sanchez, A., Oughton, D. & Rowland, A. (1997). Use of single and sequential chemical extractants to assess radionuclide and heavy metal availability from soils for root uptake. *Analyst*, 122 (8): 89R-100R.
- Kinoshita, N., Sueki, K., Sasa, K., Kitagawa, J.-i., Ikarashi, S., Nishimura, T., Wong, Y.-S., Satou, Y., Handa, K. & Takahashi, T. (2011). Assessment of individual radionuclide distributions from the Fukushima nuclear accident covering central-east Japan. *Proceedings of the National Academy of Sciences*, 108 (49): 19526-19529.
- Konoplev, A. (1998). Mobility and Bioavailability of Radiocesium and Radiostrontium of Chernobyl Origin. *DS Degree Thesis. RIARAE*: 325.
- Konoplev, A., Bulgakov, A., Zhirnov, V., Bobovnikova, T. L., Kulnyakov, L., Siverina, A., Popov, V. & Virchenko, E. (1998). Study of the <sup>137</sup>Cs and <sup>90</sup>Sr Behavior in Lakes Svyatoye and Kozhanovskoye, Bryansk Region. *Russian Meteorology and Hydrology* (11): 45-53.
- Konoplev, A., Bulgakov, A., Popov, V., Avila, R., Drissner, J., Klemm, E., Miller, R., Zibold, G., Johanson, K.-J. & Konopleva, I. (1999). Modelling radiocaesium bioavailability in forest soils. In *Contaminated Forests*, pp. 217-229: Springer.
- Konoplev, A., Avila, R., Bulgakov, A., Johanson, K.-J., Konopleva, I. & Popov, V. (2000). Quantitative assessment of radiocaesium bioavailability in forest soils. *Radiochimica Acta*, 88 (9-11): 789-792.
- Konoplev, A., Golosov, V., Laptev, G., Nanba, K., Onda, Y., Takase, T., Wakiyama, Y. & Yoshimura, K. (2016). Behavior of accidentally released radiocesium in soil–water environment: Looking at Fukushima from a Chernobyl perspective. *Journal of Environmental Radioactivity*, 151: 568-578. doi: 10.1016/j.jenvrad.2015.06.019.
- Kubota, T., Shin, M., Hamada, K. & Hitomi, T. (2015). Monitoring radioactive cesium concentration in a small agricultural reservoir in the Abukuma mountains. *Tech. Rep. Natl. Inst. Rural. Eng. Jpn.*, 217: 85-100.
- Lee, M., Lee, C. & Boo, B. (1997). Distribution and characteristics of <sup>239,240</sup>Pu and <sup>137</sup>Cs in the soil of Korea. *Journal of Environmental Radioactivity*, 37 (1): 1-16.
- Lind, O., De Nolf, W., Janssens, K. & Salbu, B. (2013). Micro-analytical characterisation of radioactive heterogeneities in samples from Central Asian TENORM sites. *Journal of Environmental Radioactivity*, 123: 63-70.

- Lind, O. C. (2006). *Characterisation of radioactive particles in the environment using advanced techniques*: PhD Thesis, Norwegian University of Life Sciences, Department of Plant and Environmental Sciences.
- Lind, O. C., Salbu, B., Skipperud, L., Janssens, K., Jaroszewicz, J. & De Nolf, W. (2009). Solid state speciation and potential bioavailability of depleted uranium particles from Kosovo and Kuwait. *J Environ Radioact*, 100 (4): 301-7. doi: 10.1016/j.jenvrad.2008.12.018.
- Lind, O. C., De Nolf, W., Janssens, K. & Salbu, B. (2013). Micro-analytical characterisation of radioactive heterogeneities in samples from Central Asian TENORM sites. *Journal of Environmental Radioactivity*, 123: 63-70. doi: <https://doi.org/10.1016/j.jenvrad.2012.02.012>.
- Longworth, G., Carpenter, B., Bull, R., Toole, J. & Nichols, A. (1998). Radiochemical Manual, ; AEA Technology plc. *Analytical Services Group: Harwell, Oxfordshire, UK*.
- Luthy, R. G., Allen-King, R. M., Brown, S. L. & Dzombak, D. A. (2004). Bioavailability of Contaminants in Soils and Sediments: Processes, Tools, and Applications. *Soil & Sediment Contamination*, 13 (2): 155.
- Mahara, Y. (1993). Storage and migration of fallout strontium-90 and cesium-137 for over 40 years in the surface soil of Nagasaki. *Journal of Environmental quality*, 22 (4): 722-730.
- Miyamoto, Y., Yasuda, K. & Magara, M. (2014). Size distribution of radioactive particles collected at Tokai, Japan 6 days after the nuclear accident. *Journal of environmental radioactivity*, 132: 1-7.
- Mukai, H., Hatta, T., Kitazawa, H., Yamada, H., Yaita, T. & Kogure, T. (2014). Speciation of Radioactive Soil Particles in the Fukushima Contaminated Area by IP Autoradiography and Microanalyses. *Environmental Science & Technology*, 48 (22): 13053-13059. doi: 10.1021/es502849e.
- Nagy, S. (2012). Chemistry and analysis of radionuclides. *Journal of Radioanalytical and Nuclear Chemistry*, 292 (1): 465-466. doi: 10.1007/s10967-011-1433-z.
- NCRP. (2006). *Cesium-137 in the Environment: Radioecology and Approaches to Assessment and Management; Recommendations of the National Council on Radiation Protection and Measurements*: National Council on Radiation Protection and Measurements, NCRP Report No. 154.
- Oomen, A., Rompelberg, C., Bruil, M., Dobbe, C., Pereboom, D. & Sips, A. (2003). Development of an in vitro digestion model for estimating the bioaccessibility of soil contaminants. *Archives of environmental contamination and toxicology*, 44 (3): 0281-0287.
- Oughton, D. & Kashparov, V. (2009). *Radioactive particles in the environment*: Springer.
- Oughton, D. H., Salbu, B., Riise, G., Lien, H., Østby, G. & Nøren, A. (1992). Radionuclide mobility and bioavailability in Norwegian and Soviet soils. *Analyst*, 117 (3): 481-486.
- Pansu, M. & Gautheyrou, J. (2007). *Handbook of soil analysis: mineralogical, organic and inorganic methods*: Springer Science & Business Media.
- Patnaik, P. (2003). *Handbook of inorganic chemicals*, vol. 529: McGraw-Hill New York.
- Pentreath, R. J. (1988). Radionuclides in the Aquatic Environment. In Harley, J. H., Schmidt, G. D. & Silini, G. (eds) *Radionuclides in the Food Chain*, pp. 99-119. London: Springer London.
- Poinssot, C. & Geckeis, H. (2012). *Radionuclide Behaviour in the Natural Environment: Science, Implications and Lessons for the Nuclear industry*. Woodhead Publishing Series in Energy: Elsevier Science.
- Pozolotina, V., Molchanova, I., Mikhaylovskaya, L., Antonova, E. & Karavaeva, E. (2012). The current state of terrestrial ecosystems in the Eastern Ural Radioactive Trace. *Radionuclides: sources, properties and hazards*: 1-22.
- Reinprecht, I., Windisch, M. & Fahnestock, M. (2002). Deterioration of storage phosphor screens with use. *Journal of Labelled Compounds and Radiopharmaceuticals: The Official Journal of the International Isotope Society*, 45 (4): 339-345.

- Rigol, A., Vidal, M. & Rauret, G. (2002). An overview of the effect of organic matter on soil-radiocaesium interaction: implications in root uptake. *J Environ Radioact*, 58 (2-3): 191-216.
- Rosén, K., Öborn, I. & Lönsjö, H. (1999). Migration of radiocaesium in Swedish soil profiles after the Chernobyl accident, 1987–1995. *Journal of Environmental Radioactivity*, 46 (1): 45-66.
- Ruby, M. V., Schoof, R., Brattin, W., Goldade, M., Post, G., Harnois, M., Mosby, D., Casteel, S., Berti, W. & Carpenter, M. (1999). Advances in evaluating the oral bioavailability of inorganics in soil for use in human health risk assessment. *Environmental Science & Technology*, 33 (21): 3697-3705.
- Saito, K., Tanihata, I., Fujiwara, M., Saito, T., Shimoura, S., Otsuka, T., Onda, Y., Hoshi, M., Ikeuchi, Y. & Takahashi, F. (2015). Detailed deposition density maps constructed by large-scale soil sampling for gamma-ray emitting radioactive nuclides from the Fukushima Dai-ichi Nuclear Power Plant accident. *Journal of environmental radioactivity*, 139: 308-319.
- Saito, T., Makino, H. & Tanaka, S. (2014). Geochemical and grain-size distribution of radioactive and stable cesium in Fukushima soils: implications for their long-term behavior. *Journal of Environmental Radioactivity*, 138: 11.
- Salbu, B. & Krekling, T. (1998). Characterisation of radioactive particles in the environment. *The Analyst*, 123 (5): 843-850. doi: 10.1039/a800314i.
- Salbu, B. (2000). Source-related characteristics of radioactive particles: a review. *Radiation Protection Dosimetry*, 92 (1-3): 49-54.
- Salbu, B. (2000). Speciation of radionuclides in the environment. *Encyclopedia of analytical chemistry*.
- Salbu, B., Krekling, T., Lind, O., Oughton, D., Drakopoulos, M., Simionovici, A., Snigireva, I., Snigirev, A., Weitkamp, T. & Adams, F. (2001a). High energy X-ray microscopy for characterisation of fuel particles. *Nuclear Instruments and Methods in Physics Research Section A: Accelerators, Spectrometers, Detectors and Associated Equipment*, 467: 1249-1252.
- Salbu, B., Lind, O. C., Børretzen, P. & Oughton, D. (2001b). Advanced speciation techniques for radionuclides associated with colloids and particles. In Bréchnac, F. & Brenda, J. H. (eds) *Radioactive pollutants - Impact on the environment*, pp. 243-260. Les Ulis Cedex A: France: Edp Sciences.
- Salbu, B., Lind, O. C. & Skipperud, L. (2004). Radionuclide speciation and its relevance in environmental impact assessments. *Journal of Environmental Radioactivity*, 74 (1): 233-242. doi: 10.1016/j.jenvrad.2004.01.008.
- Salbu, B. (2007). Speciation of radionuclides – analytical challenges within environmental impact and risk assessments. *Journal of Environmental Radioactivity*, 96 (1): 47-53. doi: 10.1016/j.jenvrad.2007.01.028.
- Salbu, B. (2009a). Challenges in radioecology. *Journal of Environmental Radioactivity*, 100 (12): 1086-1091. doi: <http://dx.doi.org/10.1016/j.jenvrad.2009.04.005>.
- Salbu, B. (2009b). Fractionation of radionuclide species in the environment. *Journal of Environmental Radioactivity*, 100 (4): 283-289. doi: 10.1016/j.jenvrad.2008.12.013.
- Salbu, B. & Skipperud, L. (2009). Speciation of radionuclides in the environment. *Journal of Environmental Radioactivity*, 100 (4): 281-282. doi: <http://dx.doi.org/10.1016/j.jenvrad.2008.12.008>.
- Salbu, B. (2011). Radionuclides released to the environment following nuclear events. *Integrated environmental assessment and management*, 7 (3): 362-364.
- Salbu, B. (2013). Speciation. In Atwood, D. A. (ed.) *Radionuclides in the Environment*: United Kingdom: John Wiley & Sons Inc.
- Salbu, B., Skipperud, L. & Lind, O. C. (2015). Sources Contributing to Radionuclides in the Environment: With Focus on Radioactive Particles. In Walther, C. & Gupta, D. K. (eds) *Radionuclides in the Environment: Influence of chemical speciation and plant uptake on radionuclide migration*, pp. 1-36. Cham: Springer International Publishing.

- Salbu, B. (2016). Environmental impact and risk assessments and key factors contributing to the overall uncertainties. *Journal of Environmental Radioactivity*, 151, Part 2: 352-360. doi: <http://dx.doi.org/10.1016/j.jenvrad.2015.09.001>.
- Salbu, B., Kashparov, V., Lind, O. C., Garcia-Tenorio, R., Johansen, M. P., Child, D. P., Roos, P. & Sancho, C. (2017). Challenges associated with the behaviour of radioactive particles in the environment. *Journal of Environmental Radioactivity*. doi: <https://doi.org/10.1016/j.jenvrad.2017.09.001>.
- Satou, Y., Sueki, K., Sasa, K., Adachi, K. & Igarashi, Y. (2016). First successful isolation of radioactive particles from soil near the Fukushima Daiichi Nuclear Power Plant. *Anthropocene*, 14: 71-76.
- Schindelin, J., Arganda-Carreras, I., Frise, E., Kaynig, V., Longair, M., Pietzsch, T., Preibisch, S., Rueden, C., Saalfeld, S., Schmid, B., et al. (2012). Fiji: an open-source platform for biological-image analysis. *Nature Methods*, 9: 676. doi: 10.1038/nmeth.2019
- <https://www.nature.com/articles/nmeth.2019#supplementary-information>.
- Schuller, P., Ellies, A. & Kirchner, G. (1997). Vertical migration of fallout <sup>137</sup>Cs in agricultural soils from Southern Chile. *Science of the Total Environment*, 193 (3): 197-205.
- Skipperud, L., Oughton, D. H. & Salbu, B. (2000a). The impact of plutonium speciation on the distribution coefficients in a sediment-sea water system, and radiological assessment of doses to humans. *Health physics*, 79 (2): 147-153.
- Skipperud, L., Oughton, D. H. & Salbu, B. (2000b). The impact of plutonium speciation on the distribution coefficients in a sediment-sea water system, and radiological assessment of doses to humans. *Health physics*, 79 (2): 147.
- Skipperud, L., Brown, J., Fifield, L. K., Oughton, D. H. & Salbu, B. (2009). Association of plutonium with sediments from the Ob and Yenisey Rivers and Estuaries. *Journal of environmental radioactivity*, 100 (4): 290-300.
- Skipperud, L. & Salbu, B. (2015). Sequential extraction as a tool for mobility studies of radionuclides and metals in soils and sediments. *Radiochimica Acta*, 103 (3). doi: 10.1515/ract-2014-2342.
- Smith, J. & Comans, R. (1996). Modeling the diffusive transport and remobilization of Cs in sediments: The effects of sorption kinetics and reversibility [J]. *Geochimica et Cosmochimica Acta*, 60 (6): 995-1004.
- Smith, J., Comans, R., Beresford, N., Wright, S., Howard, B. & Camplin, W. (2000). Pollution: Chernobyl's legacy in food and water. *Nature*, 405 (6783): 141.
- Smith, J. T., Fesenko, S. V., Howard, B. J., Horrill, A. D., Sanzharova, N. I., Alexakhin, R. M., Elder, D. G. & Naylor, C. (1999). Temporal change in fallout <sup>137</sup>Cs in terrestrial and aquatic systems: a whole ecosystem approach. *Environmental science & technology*, 33 (1): 49-54.
- Smith, J. T., Voitsekhovitch, O. V., Konoplev, A. V. & Kudelsky, A. V. (2005). Radioactivity in aquatic systems. In *Chernobyl—Catastrophe and Consequences*, pp. 139-189: Springer.
- Tessier, A., Campbell, P. G. & Bisson, M. (1979). Sequential extraction procedure for the speciation of particulate trace metals. *Analytical chemistry*, 51 (7): 844-851.
- Thiry, Y. & Myttenaere, C. (1993). Behaviour of radiocaesium in forest multilayered soils. *Journal of Environmental Radioactivity*, 18 (3): 247-257.
- UNSCEAR. (2014). *United Nations Scientific Committee on the Effects of Atomic Radiation. Sources and effects of ionizing radiation. UNSCEAR 2013 Report to the General Assembly with scientific annexes. Volume I, Annex A: Levels and effects of radiation exposure due to the nuclear accident after the 2011 Great east-Japan earthquake and tsunami*.
- Voutsas, D. & Samara, C. (2002). Labile and bioaccessible fractions of heavy metals in the airborne particulate matter from urban and industrial areas. *Atmospheric Environment*, 36 (22): 3583-3590. doi: [https://doi.org/10.1016/S1352-2310\(02\)00282-0](https://doi.org/10.1016/S1352-2310(02)00282-0).

- Wakiyama, Y., Konoplev, A., Wada, T., Takase, T., Byrnes, I., Carradine, M. & Nanba, K. (2017). Behavior of  $^{137}\text{Cs}$  in ponds in the vicinity of the Fukushima Dai-ichi nuclear power plant. *Journal of environmental radioactivity*, 178: 367-376.
- Whicker, F., Shaw, G., Voigt, G. & Holm, E. (1999). Radioactive contamination: state of the science and its application to predictive models. *Environmental Pollution*, 100 (1-3): 133-149.
- Whicker, F. W., Pinder III, J. E., Bowling, J. W., Alberts, J. J. & Brisbin Jr, I. L. (1990). Distribution of long-lived radionuclides in an abandoned reactor cooling reservoir. *Ecological Monographs*, 60 (4): 471-496.
- White, A., Handler, P. & Smith, E. L. (1968.). Principles of Biochemistry. McGraw-Hill, New York, pp. 1–815.
- Williams, T., Rawlins, B., Smith, B. & Breward, M. (1998). In-vitro determination of arsenic bioavailability in contaminated soil and mineral beneficiation waste from Ron Phibun, southern Thailand: a basis for improved human risk assessment. *Environmental Geochemistry and Health*, 20 (4): 169-177.
- Yasunari, T. J., Stohl, A., Hayano, R. S., Burkhart, J. F., Eckhardt, S. & Yasunari, T. (2011). Cesium-137 deposition and contamination of Japanese soils due to the Fukushima nuclear accident. *Proceedings of the National Academy of Sciences*, 108 (49): 19530-19534.
- Yoshida, S. & Muramatsu, Y. (1994). Accumulation of radiocesium in basidiomycetes collected from Japanese forests. *Science of the Total Environment*, 157: 197-205.
- Yoshida, S., Muramatsu, Y. & Ogawa, M. (1994). Radiocesium concentrations in mushrooms collected in Japan. *Journal of environmental radioactivity*, 22 (2): 141-154.

## Appendix 1A Results obtained for the sequential extraction

Table A 1: Activity concentration of <sup>137</sup>Cs in #13 (Bq/g)

	I	II	III	mean	std dev
<b>F1</b>	0,00	0,00	0,00	0,00	0,00
<b>F2</b>	53,94	53,46	47,98	51,79	3,31
<b>F3</b>	16,87	14,86	14,77	15,50	1,19
<b>F4</b>	28,60	27,11	26,58	27,43	1,05
<b>F5</b>	49,62	48,36	46,89	48,29	1,37
<b>F6</b>	366,15	381,73	361,13	369,67	10,74
<b>Rsd</b>	164,19	152,61	183,85	166,88	15,79
<b>Total</b>	679,37	678,12	681,20	679,56	1,55

Table A 2: Activity concentration of <sup>137</sup>Cs in #7 (Bq/g)

	I	II	III	mean	std dev
<b>F1</b>	1,40	1,29	0,94	1,21	0,24
<b>F2</b>	14,44	14,48	14,99	14,64	0,31
<b>F3</b>	6,66	6,54	6,33	6,51	0,17
<b>F4</b>	11,25	11,85	11,20	11,43	0,36
<b>F5</b>	31,38	31,49	31,73	31,53	0,18
<b>F6</b>	207,41	239,58	234,34	227,11	17,26
<b>Rsd</b>	93,45	95,26	105,22	97,98	6,34
<b>Total</b>	366,00	400,47	404,76	390,41	21,25

Table A 3: Activity concentration of <sup>137</sup>Cs in #8 (Bq/g)

	I	II	III	mean	std dev
<b>F1</b>	0,00	0,00	0,00	0,00	0,00
<b>F2</b>	2,78	2,61	2,91	2,77	0,15
<b>F3</b>	0,77	0,80	0,79	0,79	0,01
<b>F4</b>	2,49	2,42	2,98	2,63	0,31
<b>F5</b>	5,82	5,85	5,85	5,84	0,02
<b>F6</b>	102,43	111,94	118,62	111,00	8,14
<b>Rsd</b>	73,74	53,64	60,59	62,65	10,21
<b>Total</b>	188,04	177,26	191,74	185,68	7,53

Table A 4: Activity concentration of <sup>137</sup>Cs in #16B (Bq/g)

	I	II	III	mean	std dev
<b>F1</b>	0,00	0,00	0,00	0,00	0,00
<b>F2</b>	0,00	0,00	0,00	0,00	0,00
<b>F3</b>	17,30	18,10	17,48	17,63	0,42
<b>F4</b>	9,19	9,29	8,60	9,02	0,37
<b>F5</b>	7,86	9,15	8,43	8,48	0,65
<b>F6</b>	21,62	21,47	21,16	21,42	0,24
<b>Rsd</b>	24,81	108,81	113,14	82,25	49,80
<b>Total</b>	80,79	166,82	168,81	138,81	50,26

Table A 5: Activity concentration (Bq/g) of <sup>137</sup> Cs in site #16A

I	II	III	mean	std dev
<b>0,00</b>	0,00	0,00	0,00	0,00
<b>0,00</b>	0,00	0,00	0,00	0,00
<b>0,00</b>	0,37	0,30	0,22	0,20
<b>0,35</b>	0,44	0,46	0,42	0,06
<b>0,55</b>	0,61	0,84	0,67	0,15
<b>22,16</b>	24,22	22,85	23,07	1,05
<b>28,60</b>	27,45	33,15	29,73	3,01
<b>51,66</b>	<b>53,09</b>	<b>57,60</b>	<b>54,12</b>	3,10

Table A 6: Activity concentration of <sup>137</sup>Cs in #18 (Bq/g)

I	II	III	mean	std dev
<b>F1</b>	0,00	0,00	0,00	0,00
<b>F2</b>	0,00	0,00	0,00	0,00
<b>F3</b>	2,91	3,09	2,89	2,96
<b>F4</b>	2,76	3,43	2,40	2,86
<b>F5</b>	2,86	3,43	2,55	2,95
<b>F6</b>	190,90	194,50	165,09	183,50
<b>Rsd</b>	80,67	22,13	17,87	40,22
<b>Total</b>	280,10	226,58	190,80	232,49

Table A 7

Activity concentration of $^{137}\text{Cs}$ in #10 (Bq/g)					
	I	II	III	mean	std dev
<b>F1</b>	0,00	0,00	0,00	0,00	0,00
<b>F2</b>	0,00	0,00	0,00	0,00	0,00
<b>F3</b>	0,40	0,38	0,37	0,38	0,02
<b>F4</b>	0,42	0,00	0,43	0,28	0,25
<b>F5</b>	0,31	0,34	0,36	0,34	0,02
<b>F6</b>	2,68	2,32	2,17	2,39	0,26
<b>Rsd</b>	2,37	1,27	1,26	1,63	0,63
<b>Total</b>	<b>6,18</b>	<b>4,31</b>	<b>4,59</b>	<b>5,03</b>	<b>1,01</b>



**Norges miljø- og biovitenskapelige universitet**  
Noregs miljø- og biovitenskapelige universitet  
Norwegian University of Life Sciences

Postboks 5003  
NO-1432 Ås  
Norway